

*Addis Ababa
University*

(Since 1950)



ADDIS ABABA UNIVERSITY
SCHOOL OF GRADUATE STUDIES
FACULTY OF SCIENCE
DEPARTMENT OF EARTH SCIENCE

**MAPPING OF SOIL SALINITY IN SEGO IRRIGATION FARM,
SOUTHERN ETHIOPIA USING GEOSPATIAL TOOLS**

**Thesis Submitted to the School of Graduate Studies in Partial Fulfilment of the
Requirements for the Degree of Master of Science in Geo-information Science**

By: Zewdu Shegena

Advisor: Dr. K.V.Suryabhagavan

Co-advisor: Prof. M. Balakrishnan

June 2012

**MAPPING OF SOIL SALINITY IN SEGO IRRIGATION FARM,
SOUTHERN ETHIOPIA USING GEOSPATIAL TOOLS**

**Dissertation submitted for Partial Fulfilment of the Requirements for the
Award of the Degree of**

MASTER OF SCIENCE

In

**Geo-information Science of Addis Ababa University, Addis Ababa,
Ethiopia**

Under the guidance of

Dr. K.V. Suryabhagavan

Assistant Professor, Department of Earth Sciences

Addis Ababa University, Addis Ababa

Co-advisor: Prof. M. Balakrishnan

By

Zewdu Shegena

June 2012

Submitted by

.....

Student	Signature	Date
---------	-----------	------

Approved by

.....

Advisor	Signature	Date
---------	-----------	------

.....

Chairman, Dept's Graduate committee	Signature	Date
--	-----------	------

.....

Examiner	Signature	Date
----------	-----------	------

.....

Examiner	Signature	Date
----------	-----------	------

ACKNOWLEDGMENTS

First of all, I would like to thank ‘Almighty God’ who made it possible for me, to begin and finish my study successfully and also for his protection and favour in my entire life.

I express my deep sense of gratitude and indebtedness to my advisor, Dr. K.V. Suryabhagavan, who helped me from the very beginning of the research to its completion. His benevolent guidance and constant encouragement helped me to complete the research work successfully on time. I am equally indebted to my co-advisor Prof. M. Balakrishnan for his encouragement and reading the manuscript and suggested valuable comments for improvement of my thesis work.

Generation Integrated Rural Development Consultant (GIRDC) deserves special thanks for all the support provided during my study. I would also like to thank the consultant company for providing me necessary data to conduct the research successfully. I am also thankful to Segeo irrigation farm workers for providing me helpful information.

I would like to thank my friend Afework Mekeberiaaw who provided me invaluable advice that was necessary for the completion of this thesis. I also thank my class mates Abebe, Debele, Tadesse and Genemo with whom I had fruitful discussions on many scientific and technical issues during the course of this thesis work.

Words cannot express my feelings, which I have for my wife, Abiyot Teshome, my family and all my friends. I am highly indebted to them for their blessings, guidance, advice, encouragement and support.

I apologize many of my friends who helped me in various means, whom I did not mention by names. I equally appreciate and acknowledge all of them.

Zewdu Shegena

TABLE OF CONTENTS

ACKNOWLEDGMENTS	IV
LIST OF TABLES	VIII
LIST OF FIGURES	IX
ABBREVIATIONS	X
ABSTRACT.....	XI
1. INTRODUCTION	1
1.1 Background	1
1.2 Statement of the Problem.....	2
1.3 Objectives.....	2
1.3.1 General Objective.....	2
1.3.2 Specific Objectives.....	3
2. LITREATURE REVIEW	4
2.1 Overview of Soil Salinity.....	4
2.2 Remote Sensing in Mapping Soil Salinity	5
2.2.1 Direct and Indirect Mapping Methods Using Spectral Reflectance.....	5
2.2.2 Image Analysis and Visual Interpretation	6
2.3 Irrigation in Soil Salinization	7
3. METHODOLOGY	8
3.1 Description of the Study Area.....	8
3.1.1 Location	8
3.1.2 Climate	8
3.1.3 Geology.....	9
3.1.4 Soil	9
3.1.5 Land use and Land cover	10
3.2 Materials used	10
3.3 Methods.....	11
3.3.1 Salinity Mapping.....	11
3.3.1.1 Salinity Index	11
3.3.1.2 Vegetation Indicator.....	11
3.3.1.3 Soil Salinity Change Analysis.....	11
3.3.1.4 Salinity Model from Measured ECe and Spectral Reflectance	12
3.3.1.5 Soil Salinization Model.....	12

3.3.2	Overlay Analysis	13
3.3.3	Validation and Comparison of the Methods	13
3.3.4	Data Analysis	14
3.3.4.1	Data Collection and Preparation	14
3.3.4.2	Classification of Salt Affected Areas from Satellite Images	14
3.3.4.2.1	Band Selection and True and False Colour Composition	15
3.3.4.2.2	Spectral Classes of Features	16
3.3.4.3	Regression Analysis from ECe Data and NDSI	16
3.3.5	Analysis for Overlay Soil Salinity Model	18
3.3.5.1	Model Parameters	18
3.3.5.1.1	Ground water level	18
3.3.5.1.2	Landform	20
3.3.5.1.3	Land cover	22
3.3.5.1.4	Land management	23
3.3.5.1.5	Soil texture	24
3.3.5.2	Multi-Criteria decision making	25
3.3.6	Spatial Distribution of Salinity with Respect to Water Table and Soil Map	27
3.3.6.1	Water table	27
3.3.6.2	Soil types map	28
4.	RESULTS AND DISCUSSION	30
4.1	Characterization of Salt Affected Areas	30
4.1.1	Non-Saline	30
4.1.2	Slightly Saline	30
4.1.3	Moderately Saline	30
4.1.4	Strongly Saline	30
4.2	Result from Image Interpretation	31
4.2.1	Results from Supervised Image Classification	31
4.2.2	Results from Indices Analysis	34
4.3	Result of Empirical Model from Soil Salinity (ECe) and NDSI	37
4.4	Result from Overlay Salinization Model	39
4.5	Validation and Comparison of the Models	42
4.6	Distribution of Salt Affected Areas with Respect to Water Table and Soil Type	43
4.6.1	Water Table	44
4.6.2	Soil Type	44

5. CONCLUSION AND RECOMMENDATIONS	46
5.1 Conclusion	46
5.2 Recommendations	47
REFERENCES	49
APPENDIX-I.....	52
APPENDIX-II.....	54
APPENDIX-III	55

LIST OF TABLES

Table 2.1 USDA classification of salt affected soils.....	5
Table 3.1 Data type and sources	10
Table 3.2 Classification of water table depth.....	20
Table 3.3 Pair-wise comparison of factor layers.....	26
Table 3.4 Principal eigenvector of the pair-wise comparison matrix.....	27
Table 3.5 Classification of water table depth.....	27
Table 4.1 Land cover class and change rate for the years (1984, 1995 and 2010)	33
Table 4.2 Proportion of land cover converted from each class during (1984 - 2010).....	33
Table 4.3 Soil salinity class derived from NDSI and change rate for 1984, 1995 and 2010	35
Table 4.4 Proportion of salinity that was converted from each class to the rest during 1984 to 2010...35	
Table 4.5 Area extent of soil salinity level derived from empirical model.....	38
Table 4.6 Area extent of salinity classes derived from overlay model	40
Table 4.7 Soil salinity distribution with respect to water table depth	44
Table 4.8 Soil salinity distribution with respect to soil type.....	45

LIST OF FIGURES

Figure 3.1. Location map of the Study Area.....	8
Figure 3.2. Average monthly rainfall in the study area.....	9
Figure 3.3. Methodology flow chart	14
Figure 3.4 False colour composite of 2010 Landsat image.....	15
Figure 3.5 Spectral profile for land covers classes.....	16
Figure 3.6. Distribution of ECe sample points.....	17
Figure 3.7. Ground water table location map.....	19
Figure 3.8 Interpolated ground water level	20
Figure 3.9 Reclassified ground water level.....	20
Figure 3.10 Digital elevation model.....	21
Figure 3.11 Reclassified landform	22
Figure 3.12 Land cover of the study area based on vegetation density.....	23
Figure 3.13 Land management types map of the study area.....	24
Figure 3.14 Classified soil texture map.....	25
Figure 3.15 Map of ground water level of the study area	28
Figure 3.16 Soil type map of the study area.....	29
Figure 4.1 Land cover maps of 1984, 1995 and 2010.....	32
Figure 4.2 Area of land cover class from supervised classification (1984, 1995 and 2010).....	34
Figure 4.3 Salt affected areas derived from NDSI for 1984, 1985 and 2010.....	36
Figure 4.4 Area (%) of salt affected soils derived from NDSI for 1984, 1995 and 2010	37
Figure 4.5 Regression analyses model between ECe and NDSI.....	37
Figure 4.6 Areal extent of salt affected soils derived from empirical model	38
Figure 4.7 Salt affected soil map from empirical model.....	39
Figure 4.8 Area extent of salt affected soils from overlay model	41
Figure 4.9 Salt affected soil map from overlay model	41
Figure 4.10 Correlation between measured ECe and ECe from empirical model	42
Figure 4.11 Correlation between measured ECe and raster value from overlay model (salinity level).....	43

ABBREVIATIONS

DEM	Digital Elevation Model
E	East
ECe	Saturation extracts Electrical Conductivity
ESP	Exchangeable Sodium Percentage
FCC	False Colour Composite
GCP	Ground Control Points
GIRDC	Generation Integrated Rural Development Consultant
GIS	Geographic Information System
GPS	Global Positioning System
ha	Hectare
LF	Leaching Fraction
mS/cm	Milisiemens per centimetre
N	North
NDSI	Normalized Difference Salinity Index
NDVI	Normalized Difference Vegetation Index
OWWDSE	Oromia Water Works Design and Supervision Enterprise
RGB	Red, Green, Blue
SNNP	Southern Nations and Nationalities and Peoples
STRM	Shuttle Radar Topography Mission
TCC	True Colour Composite
TM	Thematic Mapper
USA	United State of America
USDA	United State Department of Agriculture
UTM	Universal Travers Mercator
yr	Year

ABSTRACT

Salinization is the major problem of the irrigated agriculture in arid and semi-arid areas, which adversely reduce the productivity of agricultural lands. Managing salinity so as to minimize its environmental impact is a prerequisite for the long-term sustainability of irrigated agriculture. The main objective of this study was to assess the level of salinity in Sego irrigated farm and to map temporal and spatial distribution of salt affected soils to aid further management. The study employed normal image classification and developing models from NDSI versus ECe and from different thematic layers to map soil salinity using geospatial tools. Classification for Landsat image of 1984, 1995 and 2010 showed that land under intensive cultivation has significantly decreased in the 26 years period where 13 ha is put under fallow per year. The analysis of NDSI shows also the strongly saline soils have increased by 6 ha/yr. Empirical model was developed from ECe vs NDSI of 2010 image using regression analysis and it has shown coefficient of relation of 66%. The model was extended for the whole area and it has revealed that 2.0 % of the study area is strongly saline where 54.7 % of the area is non-saline. Overlay model was also developed from water table, landform, land management type, soil texture and land cover and the result showed about 26.6 % of the study area is non-saline where 39.5 % and 2.8 % is moderately and strongly saline respectively. Validation of the models was made to test their predication capability and hence overlay model has revealed better correlation coefficient of 68.0 % to the measured ECe. The map of salt affected soils derived from the overlay salinity model was used to assess the distribution of salt affected soil with respect to water table and soil type. The result showed that most of the salt affected areas are on shallow water table where the strongly saline soil accounting to 2.8 % is on the shallow water table. The distribution of salt affected area with respect to soil type shows that Cambisols and Fluvisols are greatly affected by salinity where Salonchaks and Solonetz are almost found on salt affected areas. Generally the result indicates that geospatial tools are efficient and feasible techniques for detecting salt affected areas from satellite images and different thematic maps.

Keywords: Salinization, NDSI, Geospatial tools, Empirical model, Overlay salinity model

1. INTRODUCTION

1.1 Background

Soil salinization is becoming an increasing problem, especially in arid and semi-arid regions wherever irrigation is practiced. Soil degradation due to salinity and sodicity is increasing at an alarming rate of endangering the environment, agricultural ecosystems and human life (Ali Reza, et. al., 2008). Soil salinity has resulted in limiting natural resources and agricultural land use. It is a severe environmental hazard that impacts the growth of many crops. Salt affected areas are extended on all the continents. Statistics about the extent of world salt affected areas vary; however, general estimates are close to 1 billion hectares, which represent about 7% of the earth's continental extent. More than 120 countries are confronted, to a smaller or to a greater degree with the problem of soil salinity (Al-Khaier, 2003).

Land degradation, which is the product of a complex interaction of many variables, reduces the current and/or potential capability of soil to produce goods and services. Semi-arid regions are under high pressure to supply the required food for their rapidly increasing populations. The consequent changes in land use mainly due to the policies of agricultural intensification, together with the harsh climatic conditions including global climate change, have accelerated land degradation process, which has already caused yield reduction in many parts of the arid world. Therefore, the need for detecting the occurrence of land degradation while assessing its severity at any given time becomes vital. According to Beshir and Bekele (2007), some of the problems of large scale irrigation systems in Ethiopia are the lack of awareness of the farm officials on one hand and policy problems on the other hand, and these irrigation systems with lots of problems. Irrigation systems are affected by water logging, deterioration of canal capacity and salinity.

The main source of salinity are shallow ground water tables, natural saline seeps irrigation waters, source from marine origin and intensive use of chemicals in agricultural practices. In arid and semi-arid regions where evaporation exceeds precipitation causes the upward movement of dissolved alkaline salts from ground water. At the same time, the movement of rain water causes a downward movement of the salts. The net result is the deposition of the translocated cations at or very near the soil surface which is root zones of most plants. Countries like Ethiopia where arid and semiarid climatic zones occupy over 60% of the total

area, development of technology to control and mitigate salinity and sodicity is particularly an important issue for modern agricultural management (OWWDSE, 2007).

According to the Ethiopian Irrigation Development Program, 26 medium and large scale irrigation projects are planned to be implemented. Due to topographic reasons, most of the already established or proposed large scale irrigation schemes are found in the lowlands of Ethiopia where major river basins such as Awash, Blue Nile, Wabe Shebelle river basin and Rift valley basin are located. Over 11 million ha of land in the arid, semi-arid and desert parts of Ethiopia is known to be salt affected (Loiskandl, et. al., 2007). Large areas of the Awash River Basin especially the middle and lower parts of the basin are saline or sodic or in saline sodic phase and thus potentially exposed to salinization and sodicity.

1.2 Statement of the Problem

Detection of soil degradation by means of a conventional soil survey requires a great deal of time, but remote sensing techniques offer the possibility for mapping and monitoring these processes more quickly and economically. However, to assess the accuracy of the ability of satellite images to map and monitor salinity, it is necessary to compare them with field measurements of salinity (El-haddad and Garcia, 2006). The feasibility soil survey study of the Sego command area by HALCROW-GIRDC (2009) assessed field E_{Ce} and pH and explicit some indication of soil salinity and sodicity problem. The study also identified the soil type solonchaks and solonetz, which are associated with salinity and sodicity. However, the two soil types reflect the very salty and sodic soils. Hence, mapping salinity and sodicity at different levels with the application of remote sensing and geographic information system and validating with field test data are important for irrigation management and monitoring of changes in salinity as a result of irrigation development.

1.3 Objectives

1.3.1 General Objective

- The general objective of this study was to assess the level of salinity in Sego irrigated farm and to map the distribution of the problem restricting optimum production of the area, which are useful for effective management and relevant ameliorative strategies of the problem.

1.3.2 Specific Objectives

- To assess the effect of irrigation on soil salinity change during the period from 1984 to 2010
- To detect salt affected areas in Sege irrigation farm with application of salt indices
- To develop different salinity mapping models and identify the best mapping method
- To assess the spatial distribution of salt affected soils with respect to soil types and water tables.

2. LITREATURE REVIEW

2.1 Overview of Soil Salinity

Salinization is the process by which water-soluble salts build up over the soil. This process becomes critical from an agricultural point of view, as saline soils are those which enclose neutral soluble salts in the root zone to negatively affect the development of nearly all crops. It may occur naturally or as a result of poor management practices. Irrigation modifies the balance of soil hydration by generating extra supply of water, which is associated with added salts. This results in the soil becoming salty and unproductive in the absence of rational management (Jingwei Wu, et. al., 2008). If the salinity problem cannot be remediated, the land will eventually become unproductive. Soil salinity threatens the productivity of irrigated land and the livelihoods of the farmers who depend on the affected land.

Salinity and sodicity, which are commonly occurring in arid and semiarid regions cause special problem in soil and water management. Hence, they are considered separately from other chemical properties (Richard, 1991). Soil salinity refers to the surface or near-surface accumulation of salts, mainly chlorides, sulfates and carbonates of sodium, calcium and magnesium. Customarily, the concentration of these soluble salts is expressed as the electrical conductivity (EC) of a solution extracted from a water-saturated soil paste.

The definition of saline and sodic soils has been based on the E_{Ce} (electrical conductivity of the saturation extract of soil, mScm⁻¹), pHs (pH of the saturated soil paste) and exchangeable sodium percentage of the soil (ESP) values within the root zone of most crops (Richards, 1954). Soil with E_{Ce} value < 4 mScm⁻¹ is considered as salt free and salinity effect to plants is negligible. Soil with E_{Ce} value of 4-8, 8-15 and greater than 15 are slightly, moderately and strongly saline, respectively. According to USDA classification, they have different levels of effects on plant growth and yield. The effect of salinity and sodicity arise when salt concentration in the soil water are high and it is summarized in a simple three class classification of salt affected soils (Table 2.1).

Table 2.1 USDA classification of salt affected soils

Soil	ECe (mScm-1)	ESP	pH	Description
Saline soils	>4	<15	<8.5	Non-sodic soils containing sufficient soluble salts to interfere with growth of most crops
Saline sodic soils	>4	>15	<8.5	Soils with sufficient exchangeable sodium to interfere with growth of most plants and containing appreciable quantities of soluble salts
Sodic soils	<4	>15	>8.5	Soils with sufficient exchangeable sodium to interfere with growth of most plants but without appreciable quantities of soluble salts

2.2 Remote Sensing in Mapping Soil Salinity

The geographic information systems and remote sensing techniques have become tools for the purpose of identifying and classifying saline soils. Using such technique has given a good indication of accuracy, cost effectiveness, speed, and labour saving for delineating salt affected soils in the most efficient manner (Al-Mulla, 2010). Remote sensing is timely, faster than ground methods and provides better spatial coverage in mapping soil salinity. Remote sensing data can be used as an input into a Geographic Information System (GIS) for further analysis and comparison with other data (Abbas and Khan, 2007). Integration of the land and water resources and identification of the constraints/ecological problems at the micro level will help in identifying the location specific solutions through the effective use of remote sensing based resource information. The understanding of the energy interaction with soil surface is crucial to the successful interpretation of remote sensing data as well as vegetation in the planted areas. Therefore a better understanding of some physico-chemical characteristics of saline soils may be important to improve the study of soil salinity in arid regions using remotely sensed data.

2.2.1 Direct and Indirect Mapping Methods Using Spectral Reflectance

Using remote sensing, soil salinity can be mapped both directly, by reflectance from bare soil, or from the salt crust, and indirectly from vegetative coverage and health. Panah and Zehtabian (2002) explain that the spectral reflectance characteristics of the plants in arid regions may be a good indicator of salinity. Because the plant leaves may be affected by

various kinds of stresses as well as by nutrients and salinity, due to changes of internal and external structures of leaves. Spectral reflectance characteristics of non-healthy vegetation are different from healthy vegetation. Vigorous growth and type of vegetation are easily recognised in satellite images. Therefore, plant vigour and type can be used to identify the extent of soil salinity. Such areas are usually moderately to weakly saline. Saline soils with visible salt efflorescence on the soil surface are easier to map using remote sensing and are considered to be strongly saline soils.

Indirect features like landscape may help to identify the problems of soil salinity. Relative elevation is one of the most evident landscape features in relation to salinity and moisture provided by saline and shallow groundwater table. Elnaggar and Noller (2010) suggested that field observations indicate the presence of salt accumulation in low-lying landforms. Integrate environmental variables that have significant influence on the development of secondary salinization is very important. Surface geology and terrain attributes, notably elevation and slope, are critical variables in predicting soil salinity.

2.2.2 Image Analysis and Visual Interpretation

For different types of surfaces, the amount of reflected solar radiation varies with the wavelength, which makes it possible to identify various kinds of surface or classes in a satellite image and distinguish them from each other by the difference in reflectance (Khan, et. al., 2001). Salt-affected soils could easily be visually identified from the Landsat images using the false colour composite (RGB 432) and brightness and wetness indices (Elnaggar and Noller, 2010). Normalized difference salinity index (NDSI) equations can be developed to highlight saline damaged areas, as saline soils have high reflectance values in the visible range. At present, the identification and mapping of saline soil is a combination of visual interpretation of photographs, digital analysis of false colour composite (FCC) and digital analysis of surface radiation and vegetation index. All methods require ground truth information for calibration and validation. The actual use depends on the specific aim of the survey, data availability, human skill and availability of time and money.

According to Ali Reza (2008), soil salinity is one of the most complex among soil features. On the other hand, the reflection from soil surface is not related to only one soil feature in arid area as soil salinity is a complex phenomenon. Soil surface conditions such as gravelly surface

and vegetation which are resisted to salinity and crusted surface may influence the reflectance of soils. Hence remote sensing has potential to detect salt affected soils.

2.3 Irrigation in Soil Salinization

The process of soil salinization can be categorized into two types, primary and secondary. Primary salinization involves accumulation of salts through natural processes due to high salt contents in parent materials or groundwater while secondary salinization is caused by human interventions, such as inappropriate irrigation practices for example, with salt-rich irrigation water or insufficient drainage (Shrestha, 2006). A steady-state profile of salinity in the soil can be reasonably assumed under frequently applied heavy irrigation with a leaching fraction (LF) of 0.5 or more (Patel, et. al., 2002). A lower LF, longer irrigation intervals, and various irrigation methods can cause spatially varied salt concentrations in the root zone of irrigated fields. As a consequence, there will probably be higher salt build ups if rainfall or irrigation does not provide adequate leaching. In such circumstances, a steady-state salt concentration may not be reached for several years after irrigation is introduced (Meiri, 1984).

Availability of adequate good quality water is one of the most important inputs in successful crop production. As anthropogenic activities influence the role of evaporation, leading to an increase in Na^+ and Cl^- and thus total dissolved solids (TDS), the samples fall in an environment that tends towards, a semi-arid/arid climate. Features that generally need to consider for evaluation of suitable quality of groundwater for irrigation are electrical conductivity (EC), per cent sodium, sodium adsorption ratio (SAR) and residual sodium carbonate (RSC) (Ashraf, et. al., 2011). It is therefore obvious that the groundwater contribution is a significant component of water balance and should be recognized as providing part of the water needed by the crop for evapotranspiration. The most important cation and anion in ground water resources are under Ca^{2+} , Mg^{2+} , Na^+ , HCO_3^- and NO_3^- .

3. METHODOLOGY

3.1 Description of the Study Area

3.1.1 Location

The study area is situated in Southern Nations and Nationalities and Peoples (SNNP) Regional State, Gamo Gofa Zone, Arba Minch Zuria Wereda at about 24 km in the south direction from Arba Minch town being extended on both sides of Arba Minch Konso asphalt road. Geographically, it is bounded by longitude 37°25'9" - 37°30'50" E and latitude 5°48'12" - 5°54'9" N with an area coverage of 67.47 km² (Figure 3.1). This area is a flood plain bounded by Lake Chamo in the eastern and southern directions while its northern and western directions are bounded by mountains. The area is drained by Sile and Sego River which empties in to Lake Chamo.

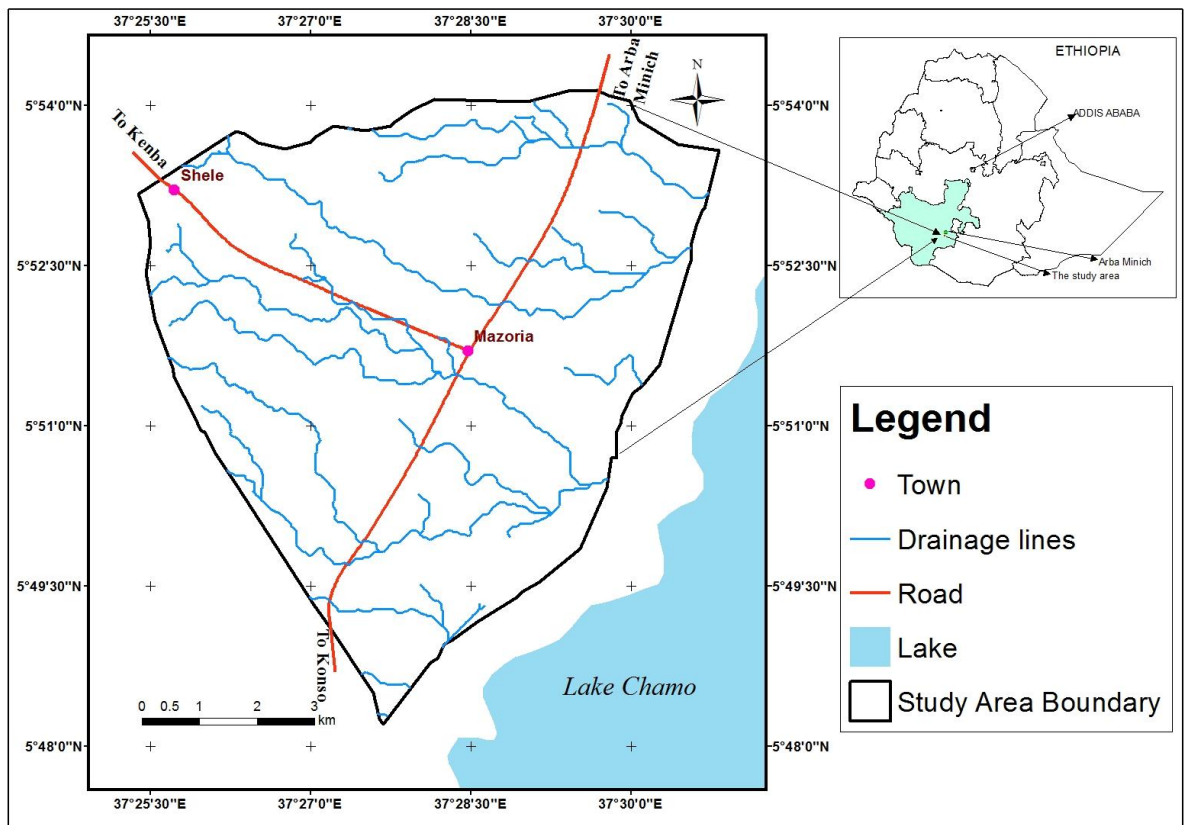


Figure 3.1. Location map of the Study Area

3.1.2 Climate

Rainfall regimes and seasons in Ethiopia are diverse. Its distribution in the study area is bimodal. A long rainy season occurs from the beginning of March to the end of May with a

maximum rainfall occurring in the month of April (219 mm); whereas a short rainy season occurs from mid-August to mid-October (Figure 3.2). The minimum monthly rainfall is recorded in January (18 mm). The study area is typically a lowland area with elevation of < 1250 m.a.s.l. Its annual evapotranspiration is almost uniformly distributed throughout the year. The seasonal temperature variation is very small. At Arba Minch close to the study site, the mean monthly temperature is 23.9°C, varying between 22.7°C in July to 25.7°C in March.

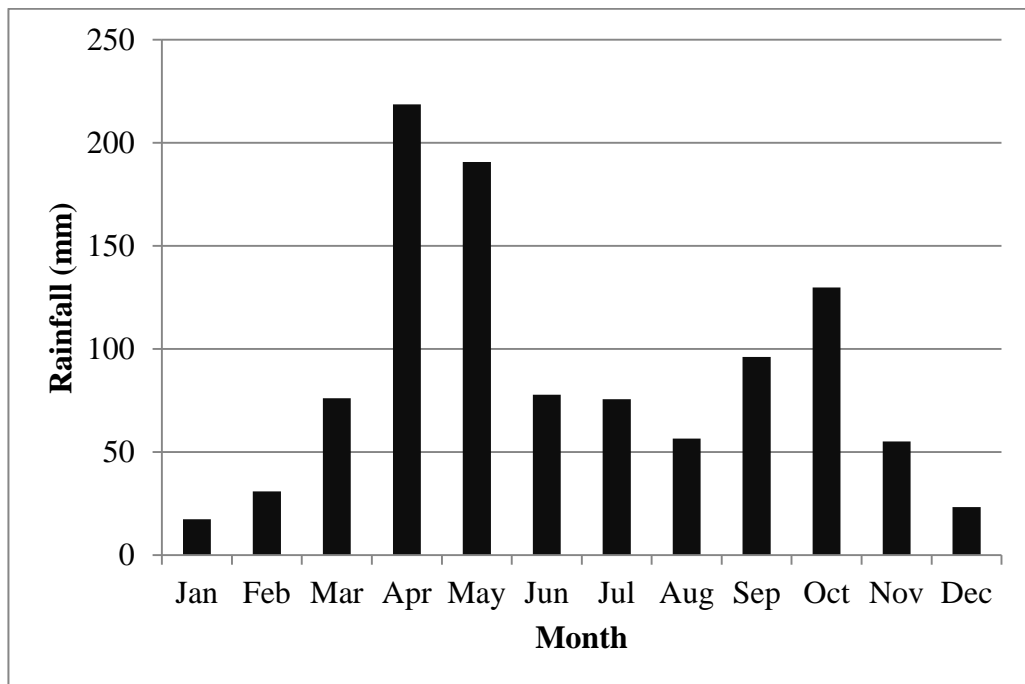


Figure 3.2. Average monthly rainfall in the study area

3.1.3 Geology

The geology of the Sego command area is characterised by lacustrine sediment; sand silt, pyroclastic deposits and diatomite. The lacustrine beds are inter-bedded with Plio-Pleistocene pyroclastics in the lakes' region and on the rift shoulders and are mostly re-deposited volcanic sands, tuff with calcareous material and diatomite (HALCROW-GIRDC, 2009).

3.1.4 Soil

The study area is mainly characterized by eight major soil types. These are Cambisols, Fluvisols, Luvisols, Vertisols, Gleysols, Solonetz, Solonchaks and Leptosols. Cambisols dominates the soil type of the area and it covers about 54% of the command area where Fluvisols takes the next part. The parent material is alluvial river deposits and colluvial materials developed over the old lacustrine deposits.

3.1.5 Land use and Land cover

The major land use/land covers of the area are dominantly intensive perennial and annual crop production. Irrigated crop production is also practised by small holders and by the state farm. Banana, cotton, mango, avocado and maize are intensively cultivated both under rain fed and irrigated conditions. The land along the river channels and periphery of Lake Chamo is used for grazing. *Accacia* and *Cordia africana* vegetation covers very few places.

3.2 Materials used

For this research the following materials were used

- Landsat TM images (path and row of 169/56 and year 1984, 1995 and 2010)
- Digital elevation model (DEM 30 meter resolution)
- Topo sheet of 1:50,000 scale (0537 A2)
- Thematic maps of soil, landforms and other maps
- Water table depth, measured field ECe and pH data and other auxiliary data
- Garmin GPS
- ArcGIS 10.0, ERDAS IMAGINE 9.2, and IDRISI Andes 32 software

Table 3.1 gives information on the sources of various materials and maps used for this study.

Table 3.1 Data type and sources

Data type		Source
Landsat TM image		Global land cover
Digital Elevation Model (DEM) with 30 m resolution		Addis Ababa University
Topo sheet of scale 1:50,000 (0537 A2)		Ethiopian Mapping Agency
GPS		Generation Integrated Rural Development Consultant
Thematic Maps	Soil type map	Generation Integrated Rural Development Consultant (GIRDC)
	Soil texture map	
	Soil ECe and pH data	
	Water table data	

3.3 Methods

To achieve the objective of the study different analysis were made which involve Remote Sensing analysis for salinity change detection, GIS assisted spatial modelling and regression analysis and finally validation and comparison of the methods.

3.3.1 Salinity Mapping

This study was aimed at determining the feasibility of using remote sensing and geographical information system to map soil salinity directly from bare soil and indirectly from vegetation and salinity change analysis using satellite images. It involves the integration of thematic layer of land management type, landform, water table level and land cover in mapping soil salinity.

3.3.1.1 Salinity Index

Soil salinity index for three Landsat images (1984, 1995 and 2010) were executed. Specifically the salinity index proposed for this study was Normalized Difference Salinity Index (NDSI). This index was derived by dividing difference of red and NIR to their sum. The mathematical formulation for NDSI is as follows:

$$\text{NDSI} = [(\text{Band 3} - \text{Band 4}) / (\text{Band 3} + \text{Band 4})]$$

3.3.1.2 Vegetation Indicator

In salinity and sodicity mapping, vegetation can be used as an indirect indicator of salt affected soils and hence stressed vegetation could be an indirect sign for the presence of salt in the soils. Salt affected soils are usually characterized by poorly vegetated areas and such state of stressed vegetation could be an indirect sign of the presence of salt in the soils. Hence vegetation index was included in the analysis and it was computed as follows:

$$\text{Normalized differential vegetation index: NDVI} = [(\text{Band4} - \text{Band3}) / (\text{Band3} + \text{Band4})]$$

3.3.1.3 Soil Salinity Change Analysis

Soil salinity changes over 26 years were analysed by mapping salt affected soils of 1984, 1995 and 2010 from Landsat TM image through supervised classification techniques and from Normalized Difference Salinity Index (NDSI). Temporal and spatial distribution of

saline soils of the area for the specified time period was assessed to infer the effect of irrigation on soil salinity rise.

3.3.1.4 Salinity Model from Measured ECe and Spectral Reflectance

Soil salinity model was developed using Landsat image of 2010 and measured ECe data. To develop the model for soil salinity levels mapping from satellite images, spectral reflectance and ECe sampling points were used. Identification of the location of sampling point on satellite image was executed. The corresponding reflectance of soil samples from different sampling zones were retrieved for different bands and indices. An empirical model for NDSI versus salinity level (ECe) was prepared using regression analysis. Figure 3.3 shows the schematic representation of the method followed.

This empirical model from NDSI has been extended for whole image and different salinity level has been identified. The advantage of this model being generalized through GIS is that it directly gives the salinity level at any point in the image.

3.3.1.5 Soil Salinization Model

There are different factors, which contribute to soil salinity as a result of their interaction. These are land management type, topography or landform, ground water level, soil texture and the reaction of the formed salt with vegetation (land cover). Hence, determining the spatial soil salinity potential of Seego irrigation farm by integrating GIS functionalities to analyse the interaction of ground water level, landform, land management type, soil texture and land cover is very crucial. The geologic formation of the command area is characterized by a single unit. However soil texture was used as one layer since grain size matters the process due to variability in texture and porosity which affects ground water flow. Therefore, the five layers; ground water level, landform, land management type, soil texture and land cover were used for soil salinization model (Figure 3.3).

Ground water is one of the factors in soil salinization by upward movement of soluble salts and accumulation at or near the soil surface. The salts present in the soil are moved with soil moisture through capillary action and become a source of saline soil formation when water table is close to the soil surface and evaporation rate is high (Chaudhry, et. al., 1996). Areas with salt accumulation are expressed with decreased vegetation as a result of reaction of vegetation with salt. The accumulation of salt near the soil surface, due to the upward

movement of salt through water, whereas the lateral movement is highly related to the low terrace (Mongkolsawat and Thirangoon, 1990).

To develop the model from the four factor layers in overlay operation in the GIS environment, map units were created which were subsequently assigned to the soil salinity potential class. In the process of the formulation of the model, reclassification was made to adjust the conditions, which are highly related to the ground truth and the existing electrical conductivity of the soil.

3.3.2 Overlay Analysis

The spatial distribution of current salt affected areas with respect to different features was assessed. This was done by overlaying map of salt affected soils with some features. The factors, which were considered in the overlay analysis, were soil type and water table.

3.3.3 Validation and Comparison of the Methods

Validation of the models was done by plotting the E_{Ce} value with the corresponding raster values of salinity map generated from satellite imagery (Empirical model) and overlay salinity model of the four map layers on scattered diagram. Then, the best fit line and equation determines the most accurate prediction of soil salinity. The validation of the models was supported by ground investigations and the existing salt crust.

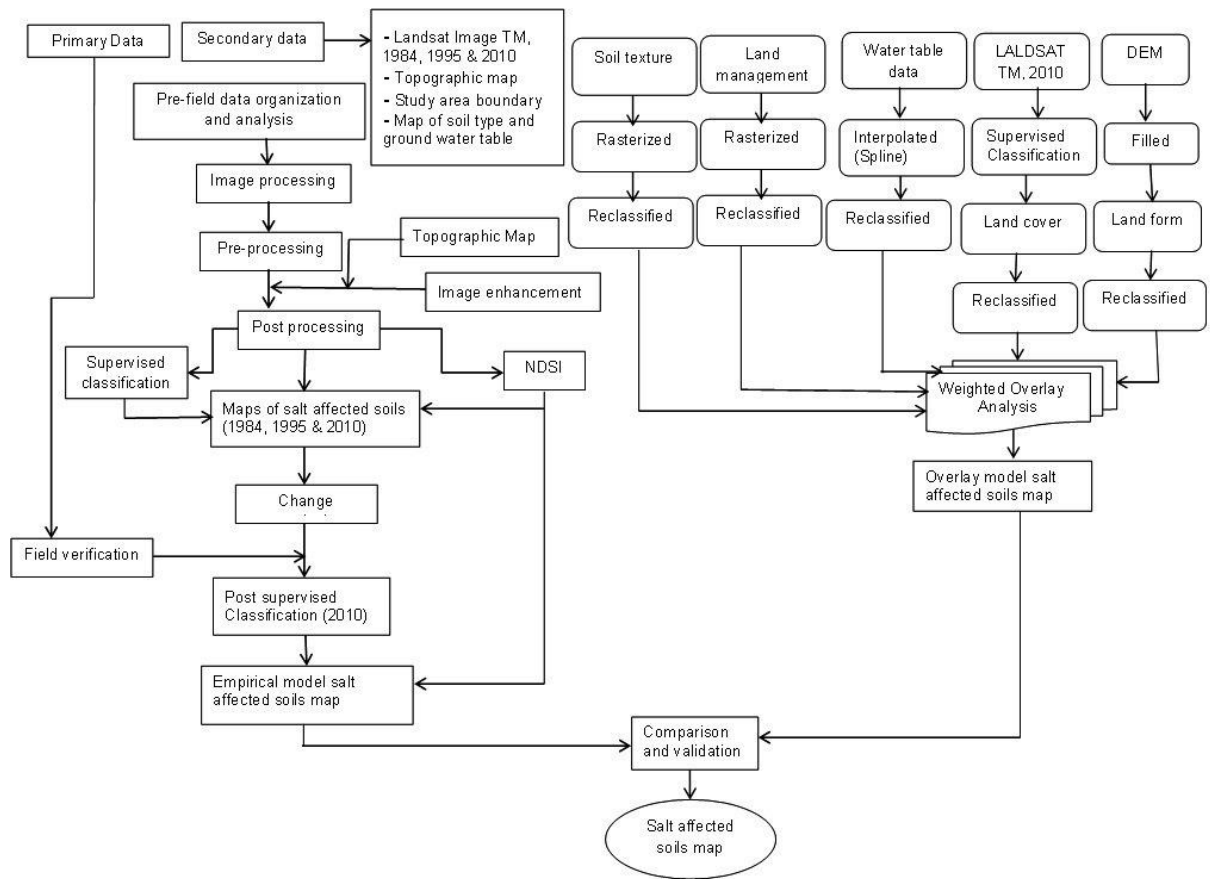


Figure 3.3. Methodology flow chart

3.3.4 Data Analysis

3.3.4.1 Data Collection and Preparation

Three Landsat images covering the period from 1984 to 2010 were acquired for the study area. Layer staking was made for all six bands excluding the thermal band. Geometric correction for the three Landsat TM images was accomplished using topographic map of the study area. The Landsat images were registered to the topographic map using control points, which were easily recognizable on the satellite image. Image enhancement was made to improve the interpretability of the images. In addition, to aid the analysis of the images, type of land use or cover was collected for 85 Ground Control Points (GCPs), with locations determined with GPS. All maps in this thesis were projected to UTM Zone 37 North using Adindan as a datum.

3.3.4.2 Classification of Salt Affected Areas from Satellite Images

An attempt was made to analyse satellite images for assessment of spatial distribution and temporal variation of salt affected soils for three different years (1984, 1995 and 2010) in this

sequence. This was done through supervised classification and normalised difference salinity index (NDSI) analysis of the Landsat TM images.

3.3.4.2.1 Band Selection and True and False Colour Composition

To increase the accuracy of image interpretation and classification of different feature class, band selection was done through the analyses of reflectance properties of features. To enhance visual interpretability of salt affected areas from the satellite image and classification of other features, various colour compositions was tested. True colour composition and other three false colour composition were found to be helpful for feature discrimination from the satellite images. True colour composition and one false colour composition (TCC: 3-2-1 and FCC: 4-3-2) were found to be the best combination for identification of different features for Landsat TM images of the three different years of the study area (Figure 3.4).

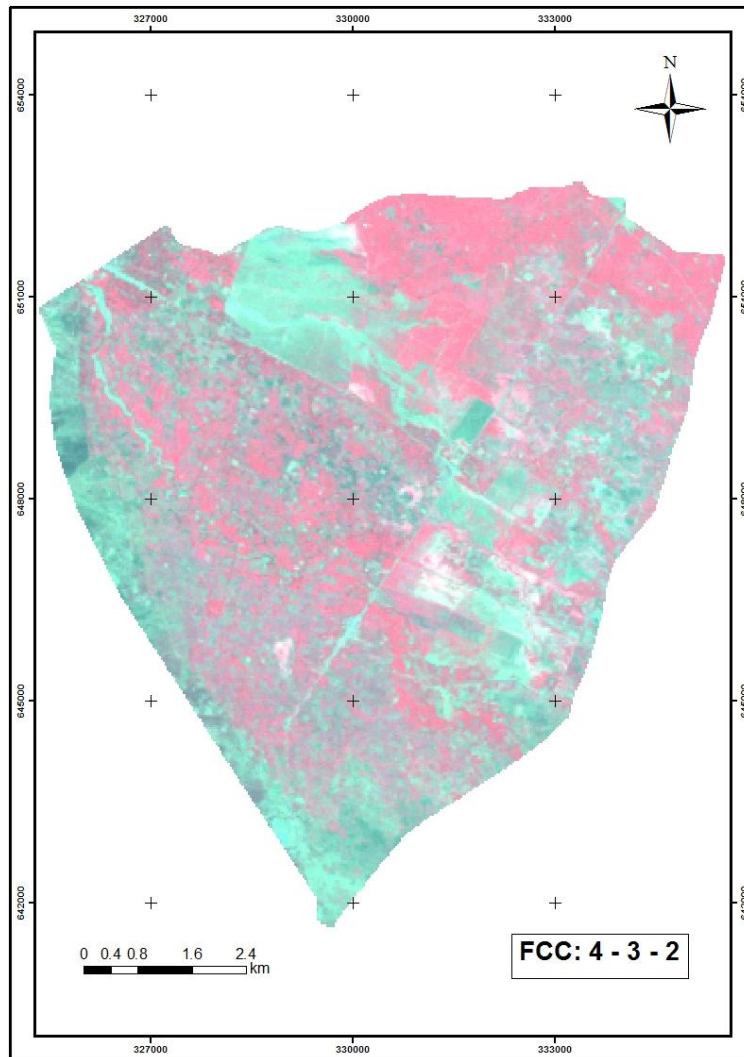


Figure 3.4 False colour composite of 2010 Landsat image

3.3.4.2.2 Spectral Classes of Features

Surface is composed of certain materials and for each material a specific reflectance curve can be established. Such curves show the fraction of the incident radiation that is reflected as a function of wave length. The spectral reflectance of soil is governed by many factors like surface soil colour, texture, mineralogy and surface vegetation cover. For the land cover classes in the study area spectral profile was generated from the satellite image using ERDAS IMAGINE 9.2 (Figure 3.5). It was observed that saline soils and bare land/fallow have similar spectral response in all the bands but saline soils had significantly higher reflectance in band 4 and band 5, which makes discrimination of saline soils and bare land easier. Dense vegetation has higher reflectance in band 4 with respect to sparse vegetation and other features.

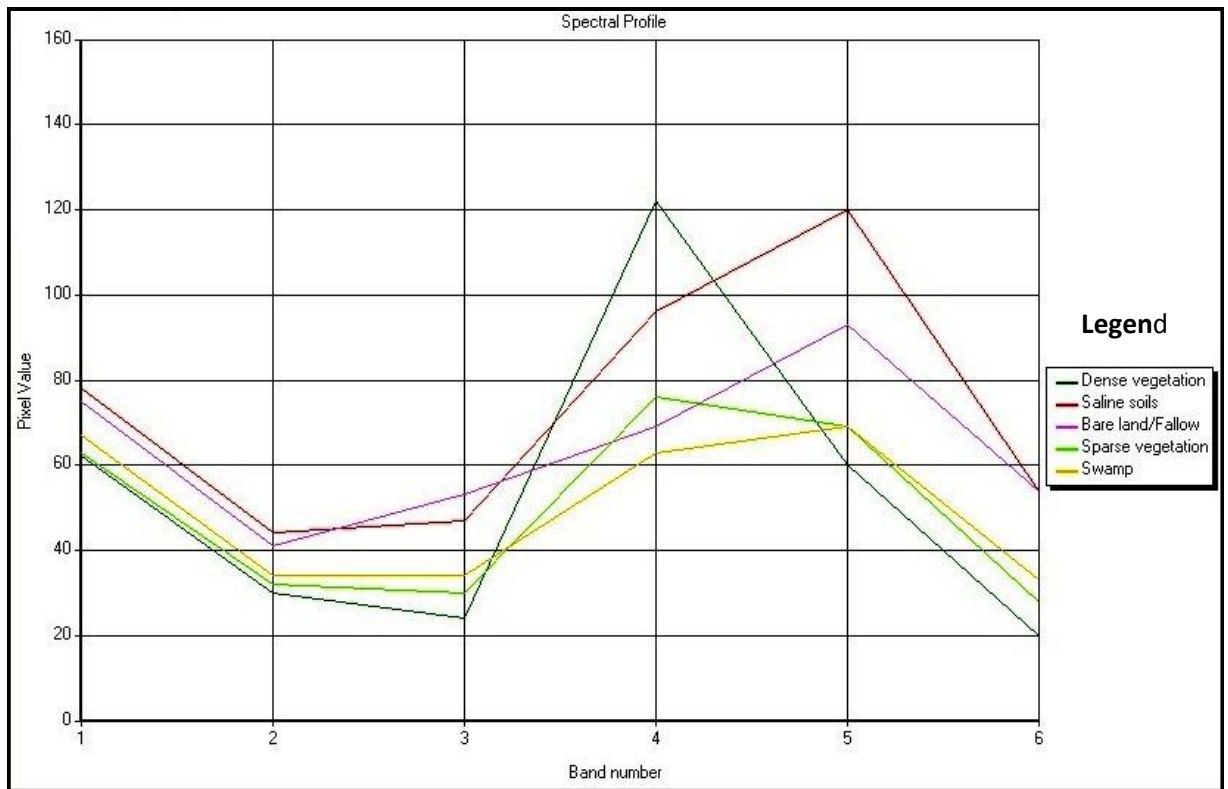


Figure 3.5 Spectral profile for land covers classes

3.3.4.3 Regression Analysis from ECe Data and NDSI

To assess the spatial distribution of ECe and to predict salinity level at different locations, regression analysis was made, which based on ECe point data and NDSI generated from Landsat image of 2010. For this analysis, a total of 84 samples ECe points were used based on the result of soil field survey by Generation Integrated Rural Development Consultant (GIRDC) in 2009. For the regression analysis, the available ECe data were acquired in 2009 and hence image of 2010 was used to generate NDSI. The best result is expected to be

obtained for this image though there is a difference of one year between the image date and ECe data acquisition and there might be slight salinity change. The distribution of ECe point data is shown in Figure 3.6.

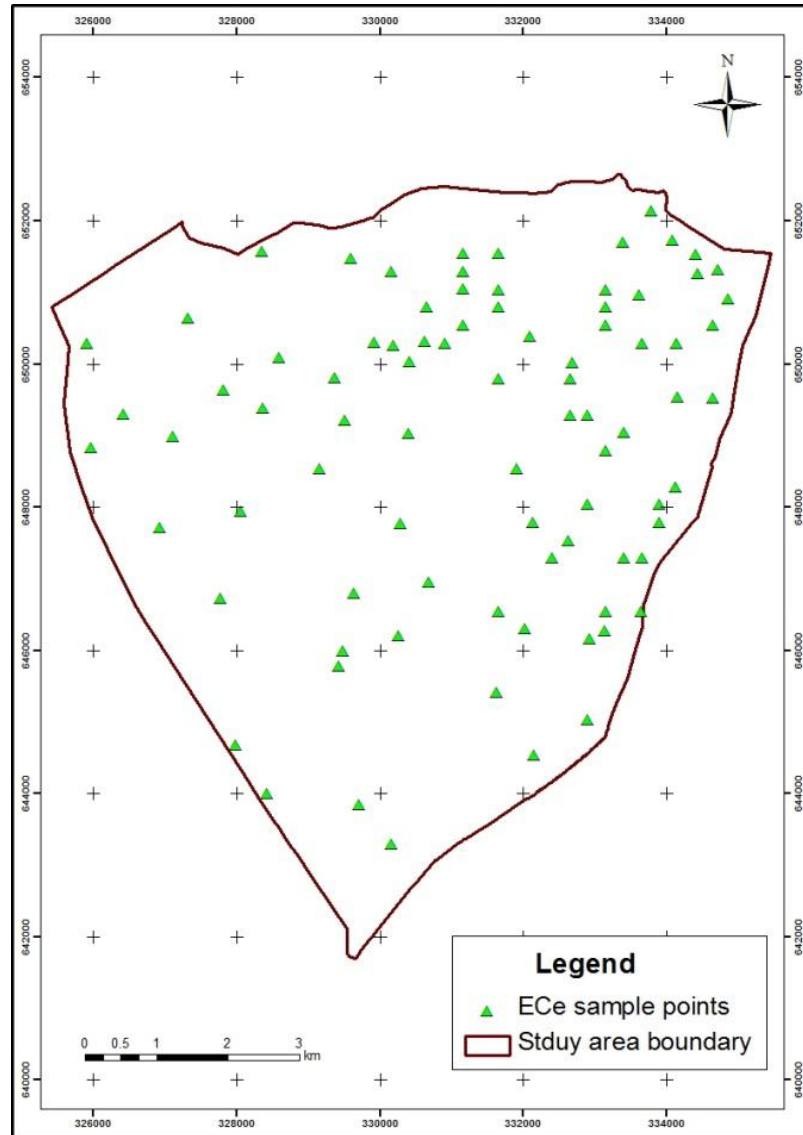


Figure 3.6. Distribution of ECe sample points

Salinity for the study area, which is expressed in ECe value, is found as point data and it represents the value at the sampling location. Attempt was made to predict the ECe values at un-sampled locations through regression analysis. This was done by distributing the ECe sample points on NDSI generated from images of 2010 in ArcMap. Then the corresponding value of NDSI for ECe point value was extracted using spatial analyst tool (Extract values to points) in ArcGIS environment. The extracted NDSI values and the corresponding ECe values were plotted on scatter diagram and the best fit line and equation were determined. Based on the equation, regression analysis model was developed using model builder in ArcGIS

environment, to predict soil salinity level for the whole area in the form of raster map. The advantage of this model generated through GIS is that it directly gives the salinity level at any point in the image and this may enhanced some new areas of strong salinity.

3.3.5 Analysis for Overlay Soil Salinity Model

The basic reason for developing models is to understand the causes of soil salinity and devise management practices required to control its spread. It is a rapid and reliable method of obtaining information on the spatial distribution of salinity (Madyaka, 2008). The effectiveness and efficiency of the method depends on the understanding of the dynamism of water and solute movement in the soil. There are several approaches for modelling soil salinization in practice, all attempting to better understand its extent and dynamics. Some of these approaches involve mathematical models, which describe and quantify the basic hydrological processes and phenomena under a range of conditions. In this study, the modelling functions include overlaying of datasets (model parameters) in GIS environment to find places, where values coincide.

3.3.5.1 Model Parameters

To develop soil salinization model, parameters were identified which have significant influence in the salinization process. These are ground water level, landform, soil texture, land-cover and type of land management. Before merging with the weighted overlay analysis, the input model parameters were first converted in to a raster data model for the five model parameters. During the conversion of the vector data in to a raster to make the data layers compatible for the raster analysis, a 30 m cell size was taken on the basis of Landsat image resolution and DEM and hence all the input parameters were resampled to 30 m raster cell size resolution. Standardization of the model parameters in to uniform scale value was made to make them compatible in the weighted overlay analysis. Each parameter was reclassified in to three salinity classes ranging from 1 to 3 on the basis of their contribution to soil salinization, where 1 implies least contributor, while 3 represents the most contributor to salinization process.

3.3.5.1.1 Ground water level

In this study, ground water level was considered as one of the parameters in the overlay analysis of soil salinization model as ground water is the most contributors in salinity rise.

Fifty one water table point data (Appendix-I) with coordinate references were acquired from GIRDC and converted in to point shape file in GIS environment (Figure 3.7).

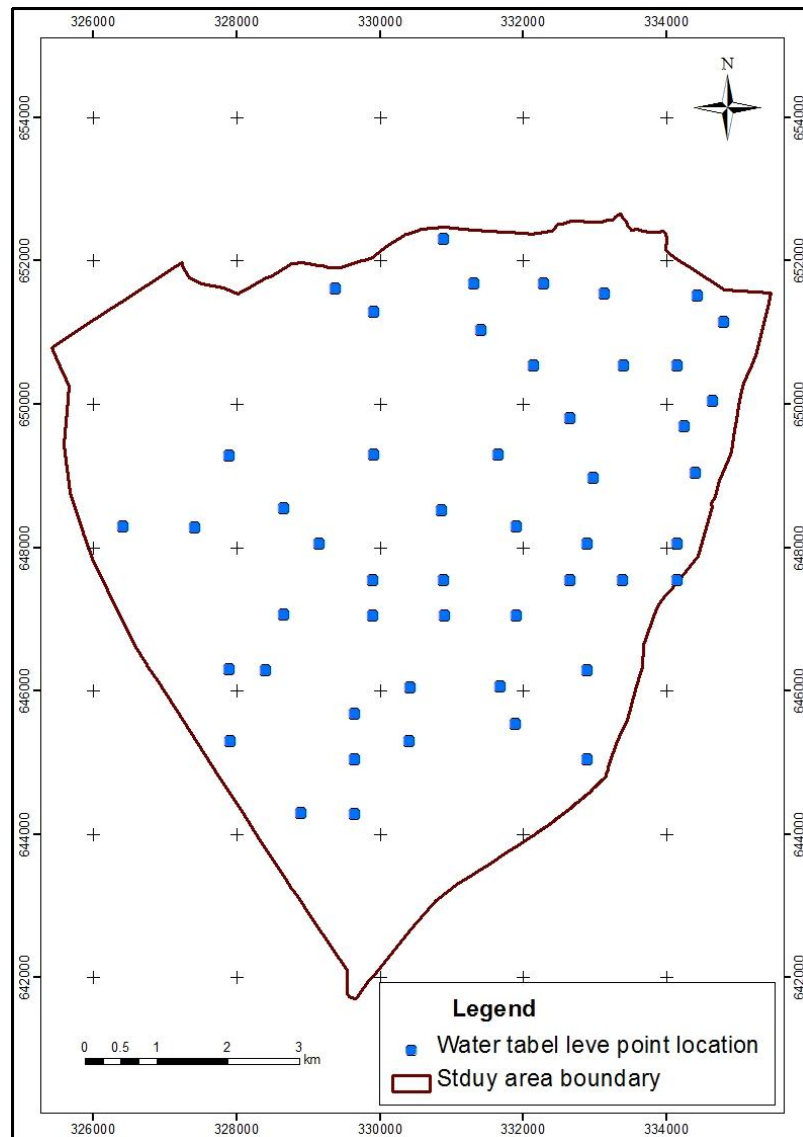


Figure 3.7. Ground water table location map

For the overlay analysis, the water table point data were interpolated to generate continuous surface water table using regularized spline interpolation in spatial analysis tools in the GIS environment (Figure 3.8). During interpolation, the raster data were sampled to 30 m cell size to make compatible with other layers in the overlay analysis. After interpolation, the continuous surface water table data were reclassified in to three classes (1 to 3) based on its contribution to the salinization process (Figure 3.9). The class 1 is the least contributor whereas class 3 is the highest contributor in the process (Table 3.2).

Table 3.2 Classification of water table depth

Water table depth (m)	Class	Contribution to salinization
0.5-2	3 (Shallow)	High
2-3	2 (Moderate)	Moderate
>3	1 (Deep)	Least

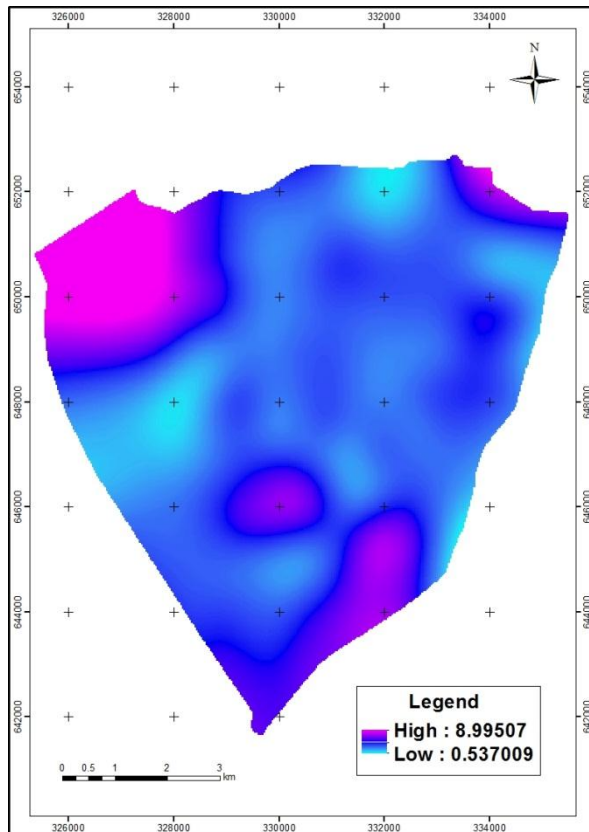


Figure 3.8 Interpolated ground water level

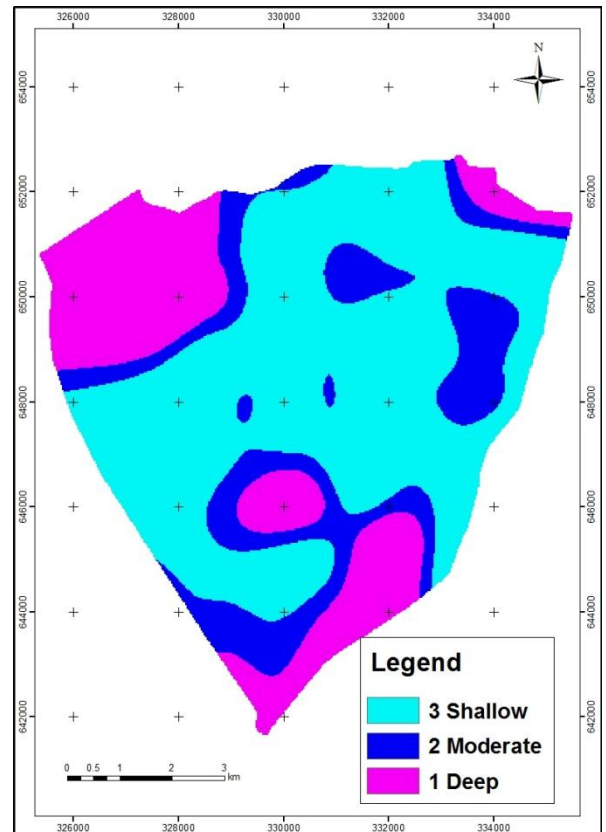


Figure 3.9 Reclassified ground water level

3.3.5.1.2 Landform

The landform of the study area was generated from 30 m resolution Digital Elevation Model (DEM) of SRTM. DEM shows that elevation of the area ranges from the lowest point near the shore of Lake Chamo to the most north western upper part of the study area which varies from 1109 to 1250 meter (Figure 3.10).

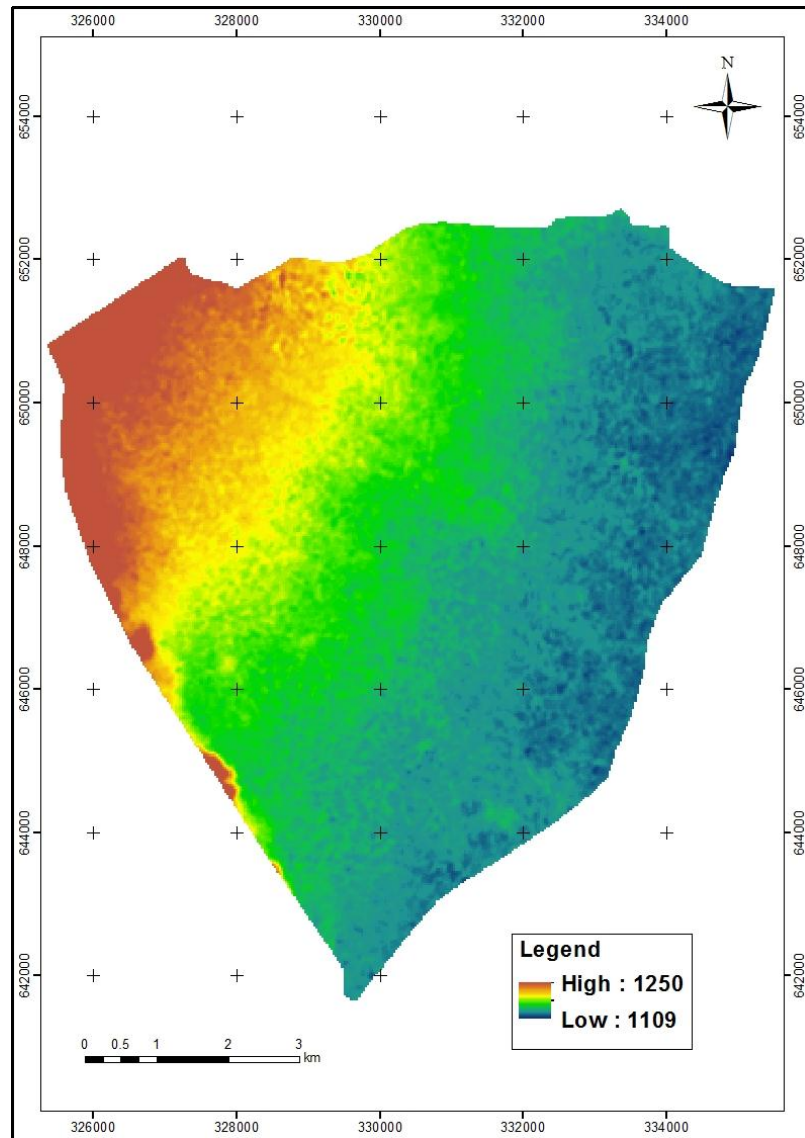


Figure 3.10 Digital elevation model

The landform of the study area was classified in to the upper and lower terrace, which was generated from digital elevation model using ArcGIS. Landform has significant importance in the process of soil salinization and hence classifying the landform and assigning proper scale value to the landform classes to make compatible with other model parameters is very important. Scale value 3 was assigned to the lower level terrace, which was very susceptible to soil salinization, where value 1 was assigned to the upper terrace and it had the least influence in the process (Figure 3.11).

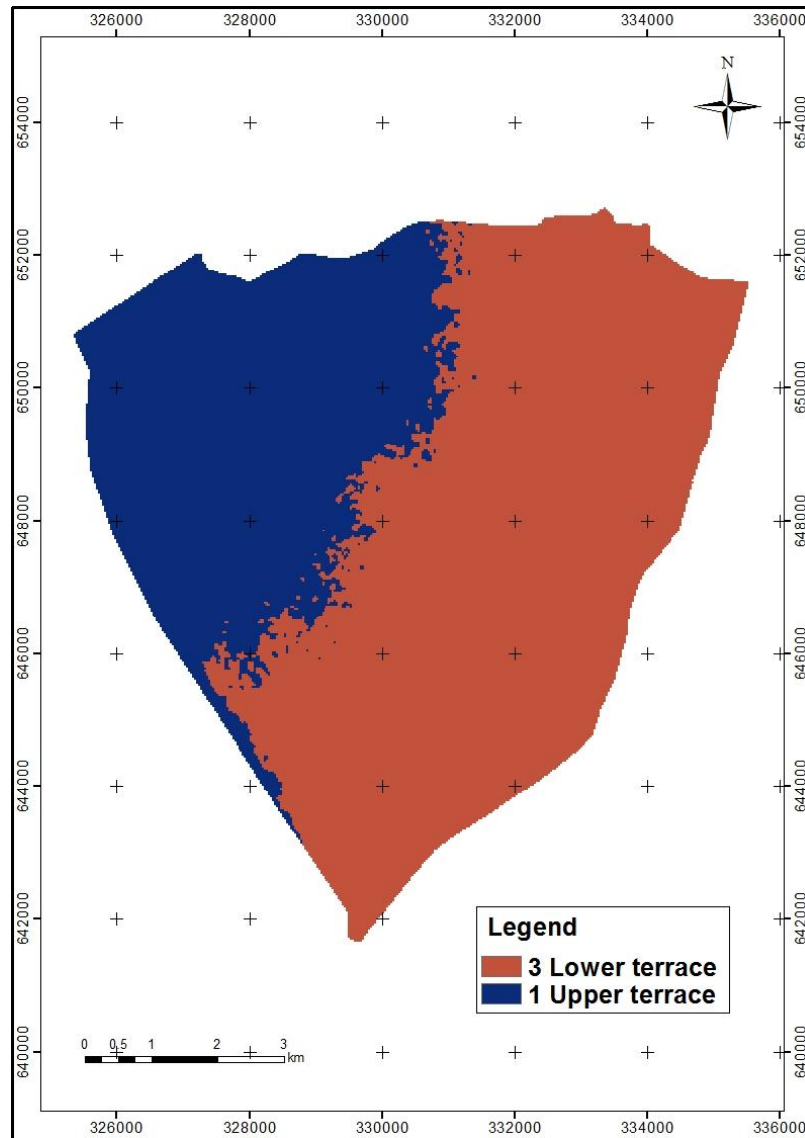


Figure 3.11 Reclassified landform

3.3.5.1.3 Land cover

The land cover was considered as one of the parameters in building soil salinization model in this research. Land cover refers to the physical state of the land surface described as the type of vegetation that covers the land. It also includes human made structures, such as buildings or pavement, and other aspects of the physical environment, such as soils and water surface. In this study, vegetation conditions were used as the main indicator of the presence and severity of saline soils. Elevated level of soil salinity affects growth of most crops as well as their appearance, and hence the state of stressed vegetation could be an indirect sign of the presence of salts in the soil. This can be detected remotely using satellite imagery where vegetation conditions can be separated into several classes from satellite images. To map vegetation density and land cover of the area from image, NDVI was generated from Landsat

image of 2010 and categorized in to three classes, as sparse, moderate and dense vegetation class, which express the density of vegetation (Figure 3.12).

The land cover derived from NDVI was reclassified and scale values were assigned to each class to make it ready for overlay analysis to be harmonious with other model parameters. The least scale value 1 was assigned to dense vegetation as salinity is less pronounced in well vegetated areas and value 2 was assigned to moderately vegetated areas (Figure 3.12). Higher value (3) was assigned to sparse vegetation as salinity is manifested on stressed vegetation.

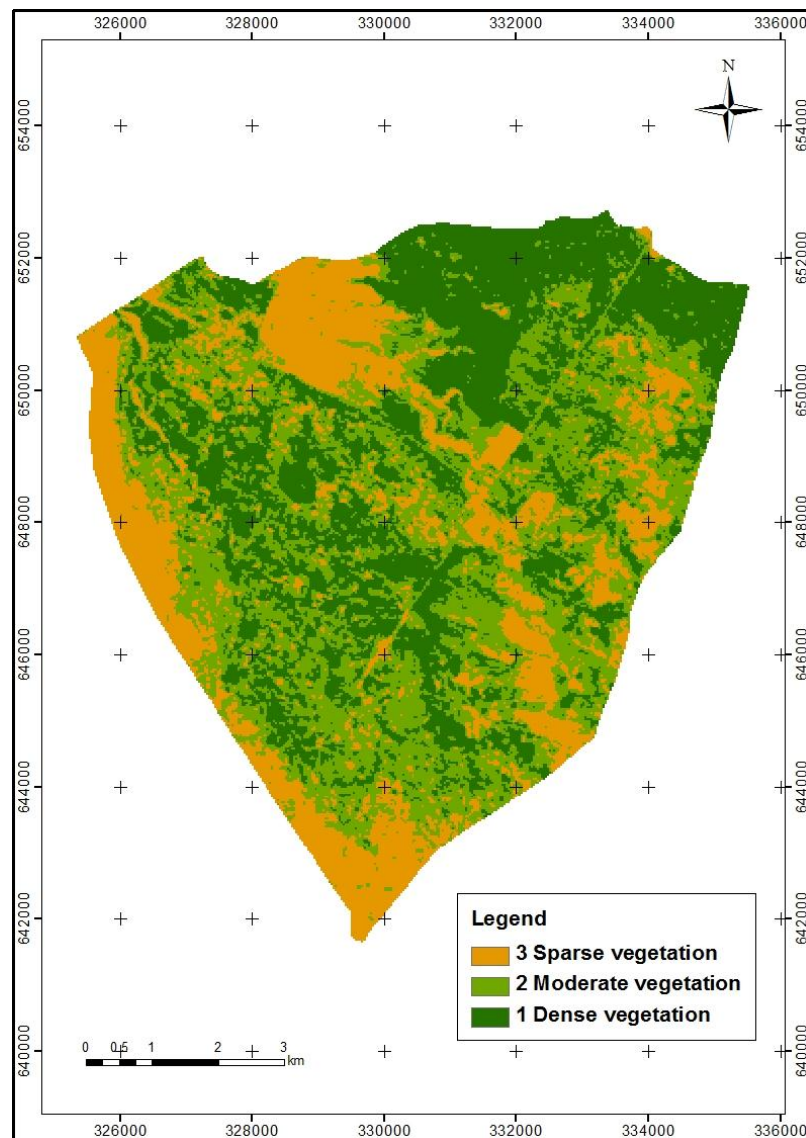


Figure 3.12 Land cover of the study area based on vegetation density

3.3.5.1.4 Land management

Land management type was considered in developing the model as lands under different level of management have different level of contribution to soil salinity. In the study area, three

land management levels were identified (Figure 3.13). These are irrigated land under state farm, mixed small holder cultivation and uncultivated land with shrub cover. Scale value 3 was assigned for land under irrigated farm as the land is susceptible to salinization due intensive irrigation water application and fertilization. Uncultivated land and mixed small holder cultivation were given scale value 1 and 2, respectively, due to their relatively lower vulnerability to salinity (Figure 3.13).

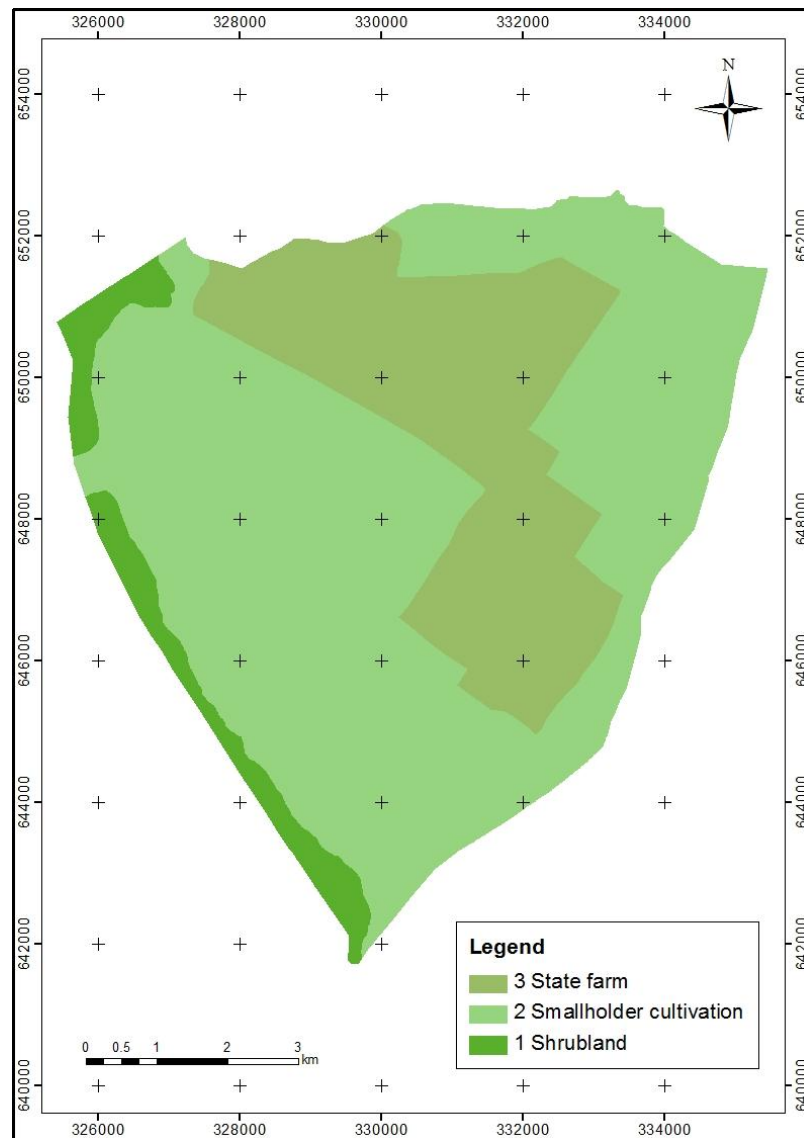


Figure 3.13 Land management types map of the study area

3.3.5.1.5 Soil texture

Another parameter affecting soil salinity is the soil particle size distribution. Generally, capillary rise is larger in a medium-textured soil than in a fine-textured soil. The surface soil salinity was more important in medium-textured soil as compared to that of fine-textured soil

(Bouksila, et. al., 2010). The soil stratification also has influence on the capillarity rise. Soils of the study area are characterized by clay, silt clay, clay loam, silt clay loam, silt loam, sandy loam and coarse gravel. For the overlay analysis this was classified in to three classes (fine, medium and coarse textured soil). Clay and silt clay was classified as fine textured soil and scale value 1 was assigned as it has low contribution to salinity where clay loam, silt clay loam and silt loam were classified as medium textured soil and scale value 3 was assigned as salinity is more pronounced in medium textured soil (Figure 3.14). Coarse textured soils (sandy loam and coarse gravel) were assigned scale value 1 as the process is less pronounced in this texture.

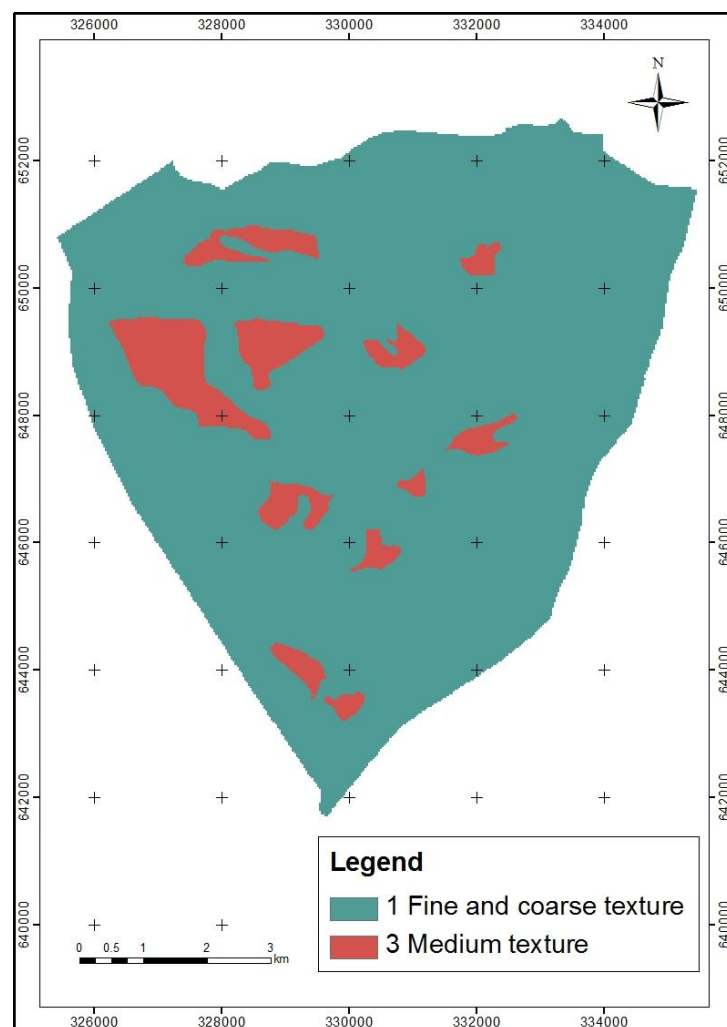


Figure 3.14 Classified soil texture map

3.3.5.2 Multi-Criteria decision making

The potential soil salinity level was obtained by creating overlay model analysis, which involved weighting of values of all data sets such as water table level, landform, land

management types, soil texture and land cover. Each criterion was weighted according to their importance in influencing soil salinization. Multi-Criteria Evaluation was used in weighted overlay analysis where weights of all the layers combined sum to one. Weightings that represent the relative importance of concerns were developed. The procedure employed to establish weight value for each layer involved in the overlay analysis was pair-wise comparisons in IDRISI Andes software version 15.0. The comparison was based on relative importance of the two criteria involved in determining salinity vulnerability of the area. Hence, every possible pairing was compared and the ratings were recorded into a pair-wise comparison matrix (Table 3.3).

Table 3.3 Pair-wise comparison of factor layers.

Layer	Water table level	Landform	Land management	Land cover	Soil texture
Water table level	1				
Landform	1/2	1			
Land management	1/2	1/2	1		
Land cover	1/3	1/2	1/2	1	
Soil texture	1/3	1/3	1/2	1/2	1

The resulting weight from pair-wise comparison for each soil salinity factors is shown in Table 3.4. The derived weight for water table level was 0.36, which indicates that water table has about 36% influences on soil salinity induction in the study area. Landform is the second factor influencing soil salinity by 25%, whereas land management, land cover and soil texture were contributing 18%, 12% and 9%, respectively. To generate map of salt affected soils from the weighted overlay analysis of soil salinization model, cell value of each model parameter was multiplied by its respective weight. Then, the resulting cell values were added to produce the final output raster, showing the level of soil salinity. To generate the final map of salt affected soils, the raster map was reclassified in to four classes, ranging from 1 to 4. In the output raster, the higher value indicates areas of strong salinity level whereas low raster value indicates less salinity level.

Table 3.4 Principal eigenvector of the pair-wise comparison matrix

Factor	Weight
Water table level	0.36
Landform	0.25
Land management	0.18
Land cover	0.12
Soil texture	0.09

3.3.6 Spatial Distribution of Salinity with Respect to Water Table and Soil Map

An attempt was made to show the spatial distribution of salt affected soil with respect to soil map and water table map. After map of salt affected soils was generated from the two models and comparison was made, the best map was taken and overlay analysis was performed with soil type and water table map to show the distribution of saline soils.

3.3.6.1 Water table

To assess the spatial distribution of salt affected soils with respect to ground water table, map of water table level was generated from water table point data acquired from GIRDC, collected in December 2008 and January 2009. The water table level point data were interpolated to draw map of water table showing areas, which are critically waterlogged, potentially waterlogged and safe (Table 3.5).

Table 3.5 Classification of water table depth

Water table depth	Risk of waterlogging
0.5-2	Critically waterlogged
2-3	Potentially waterlogged
>3	Safe area

The study by Khorasgani and Karimi (2008) show that shallow ground water table leads to high capillary movement of water and increases the risk of salinization. Based on this view, to assess the distribution of saline soils, the generated water table map (Figure 3.14) was overlaid with map of salt affected soils.

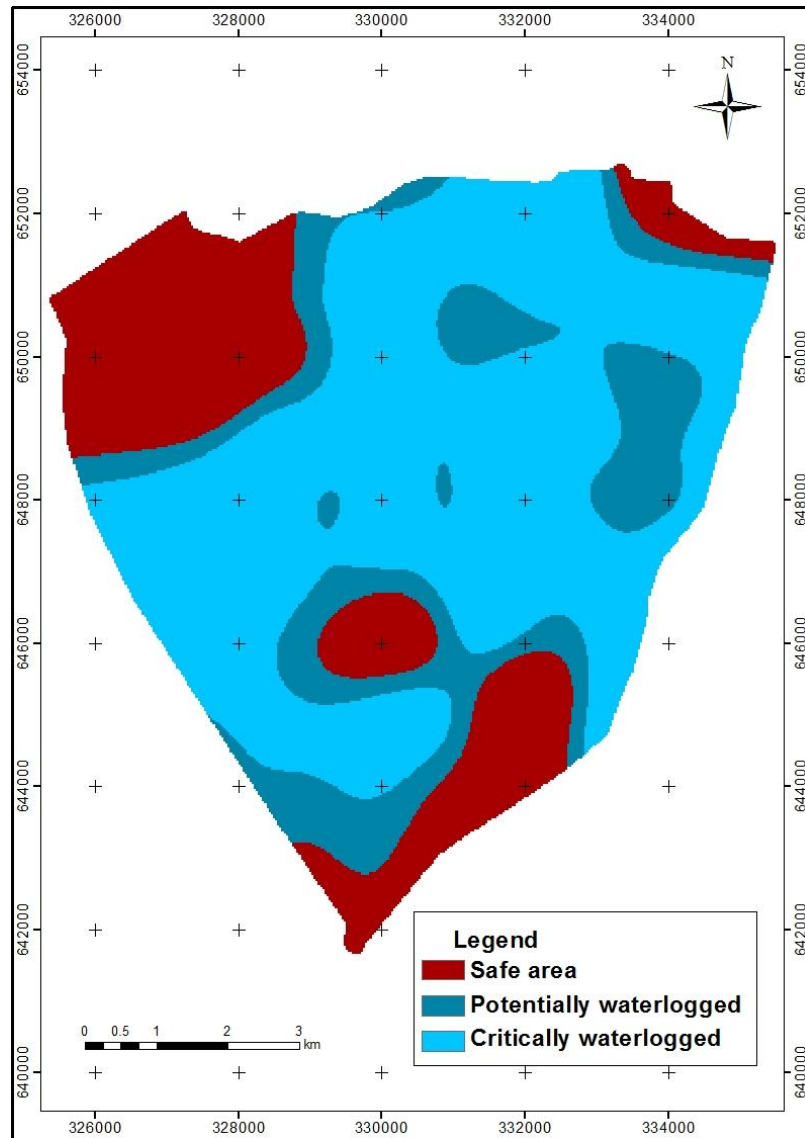


Figure 3.15 Map of ground water level of the study area

3.3.6.2 Soil types map

To assess the spatial distribution of saline soils with respect to soil type, the map of salt affected soils was overlaid with soil type map. For this purpose, map showing eight major FAO soil class with scale of 1:10,000 was obtained from GIRDC, based on the soil survey of 2009. The major soil types of the study area were Cambisols, Fluvisols, Luvisols, Vertisols, Gleysols, Solonetz, Solonchaks and Leptosols (Figure 3.15). Among these, Solonetz and Solonchaks are soils commonly occurring in arid and semi-arid region and they are associated with salinity.

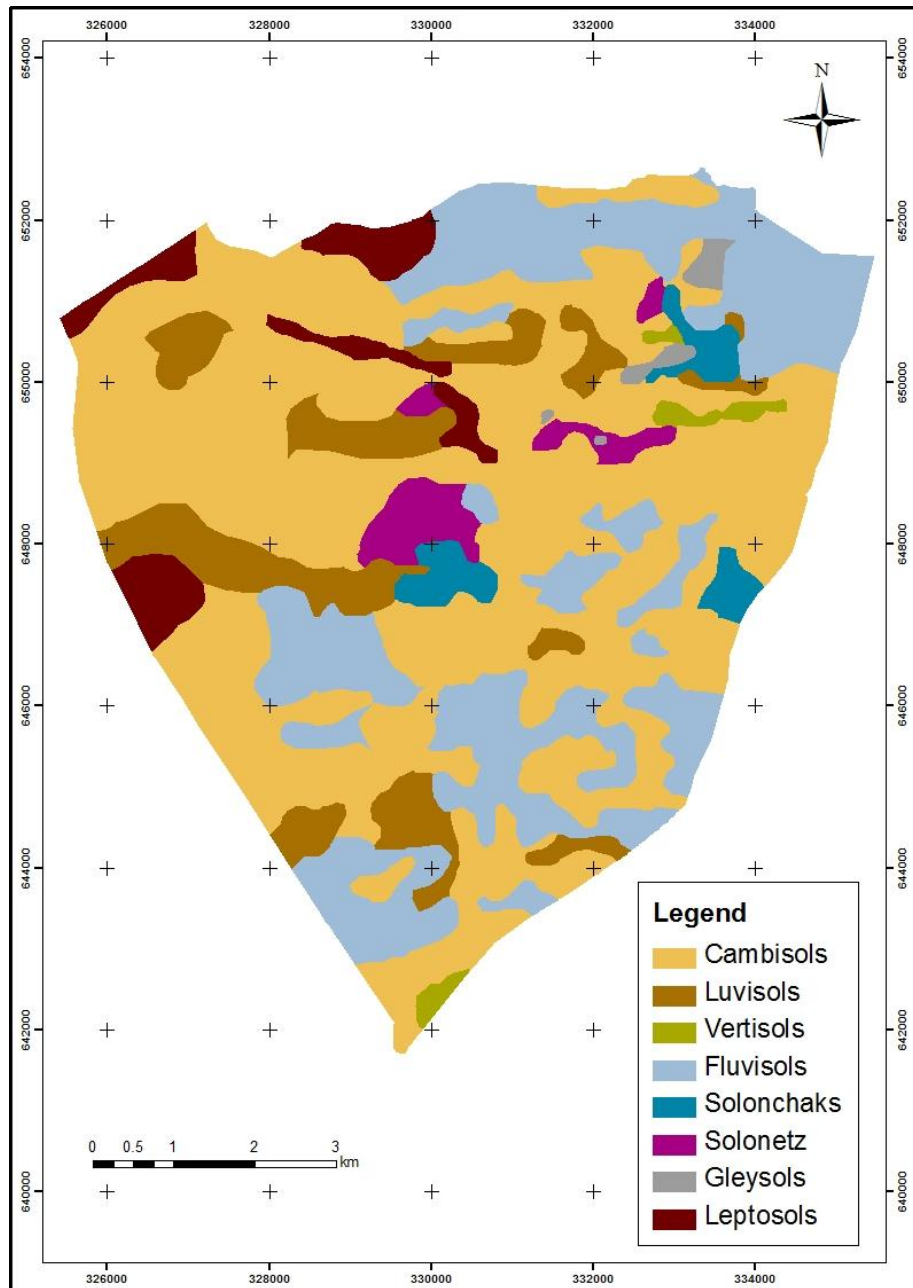


Figure 3.16 Soil type map of the study area

4. Results and Discussion

4.1 Characterization of Salt Affected Areas

The definition of saline soils has been based on the E_{Ce} values within 0-0.6m depth; this is being in the root zone of most crops. Accordingly, it is classified in to four classes of salinity level; non-saline, slightly saline, moderately saline and strongly saline with E_{Ce} values of <4 mS/cm, 4-8 mS/cm, 8-15 mS/cm and >15 mS/cm respectively. However satellite image interpretation and classification is based on the relative reflectance of features and it would not give satisfactory salinity class of salt affected areas but it can provide apparent image about the salinity status of the area.

4.1.1 Non-Saline

Non-saline soils are characterized by soil E_{Ce} of less than 4mS/cm and have no effect on the growth of most plants. On satellite images these areas were distinguished as well vegetated and normal growth of plants. The spectral reflectance profile for these areas showed high reflectance in band 4 (NIR), which is true for normal growth of plants but the amount depends on leaf development and cell structure of leaves (Bakker, et. al., 2001). These areas were identified as dark green on true colour composite or dark red on false colour composite (FCC: 4-3-2).

4.1.2 Slightly Saline

These are areas with slight salinity level with E_{Ce} values of 4-8 mS/cm. Vegetation on these areas are slightly altered due to the slight level of salt in the soils. These areas are identified as pinkish white colour on the False Colour Composite of Landsat TM image.

4.1.3 Moderately Saline

Vegetation on this soil is moderately affected and has limited growth due to the salinity level which normally ranges from 8-15 mS/cm. These areas were shown in light blue colour on the False Colour Composite.

4.1.4 Strongly Saline

Generally strongly saline soils are characterized by high level of salt in the soil (>15 mS/cm), which limits plant growth. The relative spectral reflectance of strongly saline soils is higher in

most bands. Salt affected areas were identified with bright pink colour on FCC (4-3-2). As it becomes brighter, it is difficult to differentiate from fallow or bare land.

4.2 Result from Image Interpretation

Satellite images of the different years covering a period of 26 years were analysed to have clear idea on the impact of irrigation on salinity rise. The images of 1984, 1995 and 2010 were used in the mapping of salt affected areas under supervised classification in ERDAS imagine 9.2 software where classification of 2010 image was supported by ground control points. Attempt was also made for the analysis of NDSI to extract areas of salt affected.

4.2.1 Results from Supervised Image Classification

The supervised image classification for the three different year's satellite images resulted in five land cover classes. The five land covers identified are intensive cultivation, dispersed cultivation, bare land, fallow land and water body/swamp (Figure 4.1).

In the process of classification training area was given to each of the land cover class, as based on the reflectance signature of the different feature for the band combinations (FCC: 4-3-2). To minimize classification error that arise from similar reflectance properties of features, field visit was made to collect ground control points for the recent image and informal discussion was made with the farmers to about get past history of the area for the late two image (1984 and 1995). After field visit, post classification was performed for the three images based on the information collected from the field. Then areas incorrectly classified were changed by vectorizing the previously classified image.

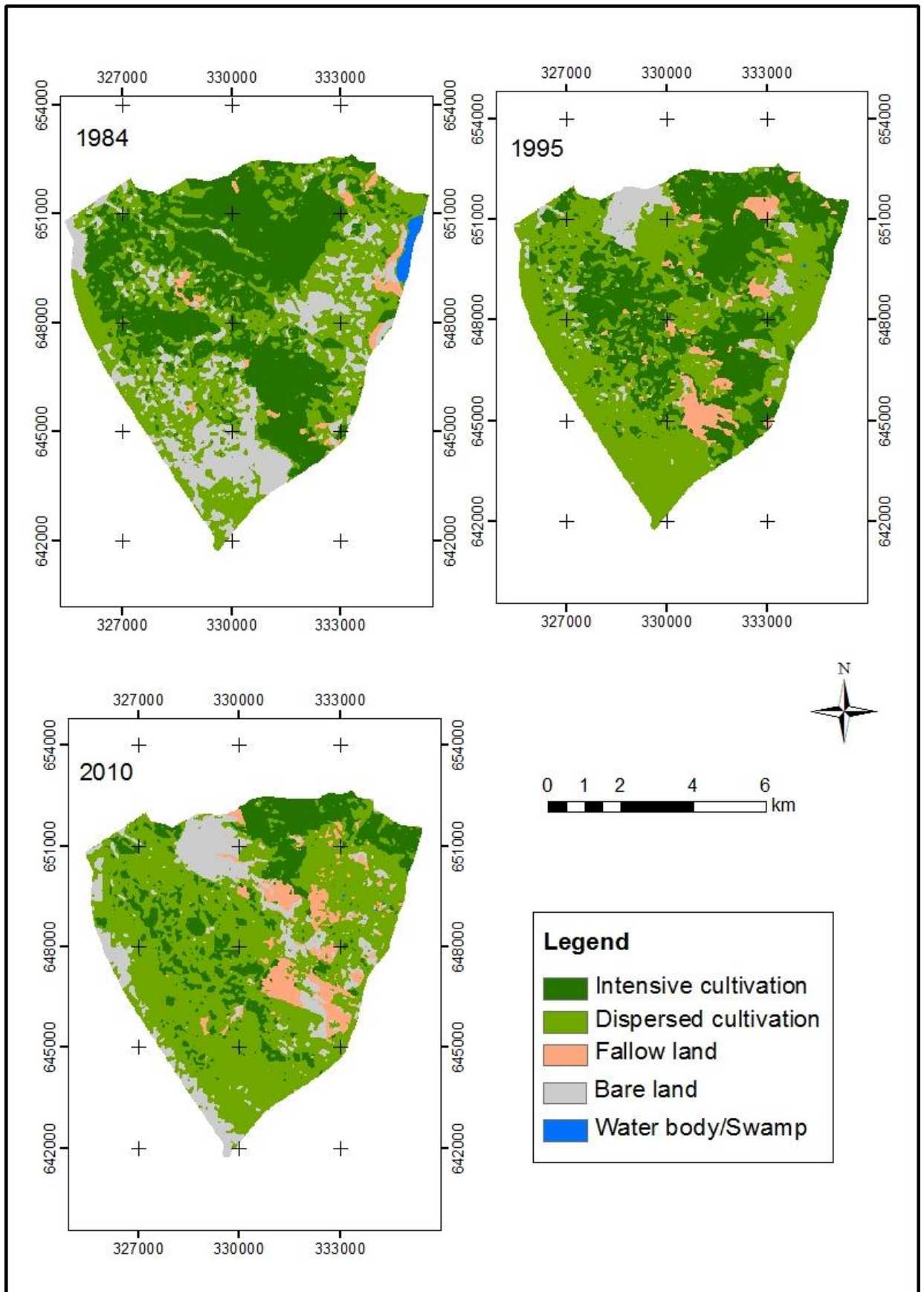


Figure 4.1 Land cover maps of 1984, 1995 and 2010

The results from supervised classification revealed that areas under intensive cultivation has decreased gradually from 40.9% to about 18.4 % of the area from 1984 to 2010 with an average rate of 3.1% per year (Table 4.1). Most of the intensive cultivation was changed to disperse cultivation and this is due to the salinity rise affecting crop growth which resulted from long term irrigation development (Table 4.2). There was a slight decrease in the extent of intensive cultivation during the period 1984 – 1995, but greater decrease was observed during 1995 - 2010. Water body along the shore of Lake Chamo, which was about 55 ha in 1984, has disappeared and swamps emerged in the middle of the farm in 1995 and 2010 accounting to 1 ha and 2 ha respectively. Area under fallow land was about 2.2 % in 1984 and this has increased to 5.6% in 1995 and further increased to 7.3% in 2010 (Figure 4.1). Areas of salt affected soils were abandoned due to its very low production as most crops have no tolerance to grow on high saline areas.

Table 4.1 Land cover class and change rate for the years (1984, 1995 and 2010)

Land use/land cover class	Year						Change/year from 1984 to 2010	
	1984		1995		2010		Change (ha)	Change (%)
	Area (ha)	Area (%)	Area (ha)	Area (%)	Area (ha)	Area (%)		
Intense cultivation	2760	40.9	2511	37.2	1244	18.4	-58	-3.1
Dispersed cultivation	2572	38.1	3451	51.1	4094	60.7	59	1.8
Bare land	1211	17.9	405	6.0	911	13.5	-12	-1.1
Fallow land	148	2.2	379	5.6	495	7.3	13	4.6
Water body/Swamp	55	0.8	1	0.0	2	0.0	-2	-13.7
Total	6747	100.0	6747	100.0	6747	100.0		

Table 4.2 Proportion of land cover converted from each class during (1984 - 2010)

	Class	Land cover type of 2010 (ha)					
		Intense cultivation	Dispersed cultivation	Bare land	Fallow land	Swamp	Total
Land cover type of 1984 (ha)	Intense cultivation	660.6	1472.1	375.5	261.2	0.0	2769.3
	Dispersed cultivation	446.5	1593.3	358.4	165.5	0.6	2564.3
	Bare land	100.8	890.5	168.4	50.6	0.3	1210.7
	Fallow land	23.5	96.6	9.4	17.5	0.6	147.6
	Water body	17.5	36.4	0.0	1.1	0.0	55.0
	Total	1248.8	4088.9	911.7	495.8	1.6	6746.9

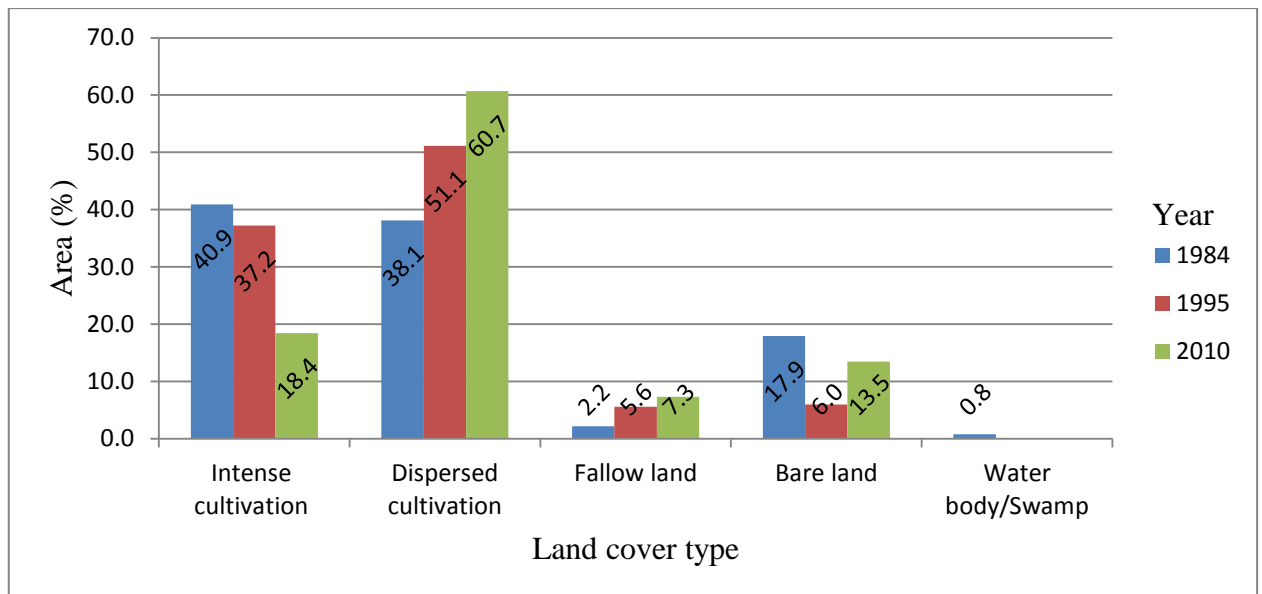


Figure 4.2 Area of land cover class from supervised classification (1984, 1995 and 2010)

4.2.2 Results from Indices Analysis

In this study NDSI for Landsat image of 1984, 1995 and 2010 was analysed for temporal and spatial detection of salt affected areas. Normalized difference salinity index was used to enhance the saline zones and suppressing the vegetation which is calculated as the ratio of the difference of red band to NIR band and divided by the summation of the two bands. The value of NDSI ranges between 1 and -1. From these areas with value 0 and less than 0 were classified as none saline. Areas with NDSI value of greater than 0 were classified as slightly saline to strongly saline and some of them as water logged. Therefore, to detect temporal variation of salt affected areas, the NDSI for images of 1984, 1995 and 2010 were classified and hence five classes were identified; non-saline, slightly saline, moderately saline, strongly saline and water body (Figure 4.3).

The result shows that about 64.9% of the areas were non-saline in 1984, which gradually decreased to 40% in 2010 (Table 4.3). Out of this 4376 ha under non-salinity in 1984, only 1976 ha remained as non-saline, whereas the rest 2400 ha areas were converted to slightly saline, moderately saline and strongly saline with a large area converted to slightly saline (Table 4.4). Large area change was observed in the strongly and moderately saline soil. Moderately saline soil was about 7.6% in 1984, which has increased to 13.6% and 22.0% in 1995 and 2010, respectively (Figure 4.4). This is with an average rate of 4.1% increase per year in the 26 years period. Strongly saline soils has increased at a rate of 5.5% per year (6 ha/yr), where a large area change was observed in the time period 1995 to 2010. Map of salt

affected soil for the three different years revealed that moderately and strongly saline soils were concentrated in the central and largely in the eastern part of the study area, along the side of Lake Chamo. This indicates that the lake may contribute to the salinity of the area through ground water rise. Water body (part of Lake Chamo) accounting to 53 ha which was detected in the image of 1984 has disappeared in the image of 1995 and 2010. This has largely converted to non-saline and slightly saline areas as some areas to moderately and strongly saline soils.

Table 4.3 Soil salinity class derived from NDSI and change rate for 1984, 1995 and 2010

Soil salinity class	Year						Change/year from 1984 to 2010	
	1984		1995		2010		Change (ha)	Change (%)
	Area (ha)	Area (%)	Area (ha)	Area (%)	Area (ha)	Area (%)		
Non-saline	4376	64.9	3979	59.0	2702	40.0	-64	-1.9
Slightly saline	1755	26.0	1777	26.3	2360	35.0	23	1.1
Moderately saline	514	7.6	916	13.6	1485	22.0	37	4.1
Strongly saline	48	0.7	75	1.1	200	3.0	6	5.5
Water body	53	0.8	0	0.0	0	0.0	-2	
Total	6747	100.0	6747	100.0	6747	100.0		

Table 4.4 Proportion of salinity that was converted from each class to the rest during 1984 to 2010

		Soil salinity in 2010 (ha)				
Salinity class		Non-saline	Slightly saline	Moderately saline	Strongly saline	Total
Soil salinity in 1984 (ha)	Non-saline	1976.1	1395.3	893.7	110.5	4375.5
	Slightly saline	556.7	695.8	439.7	63.9	1756.2
	Moderately saline	136.7	225.7	133.0	20.2	515.6
	Strongly saline	12.9	18.4	13.3	1.8	46.4
	Water body	25.7	21.8	5.0	0.5	53.1
	Total	2708.2	2357.1	1484.7	196.9	6746.9

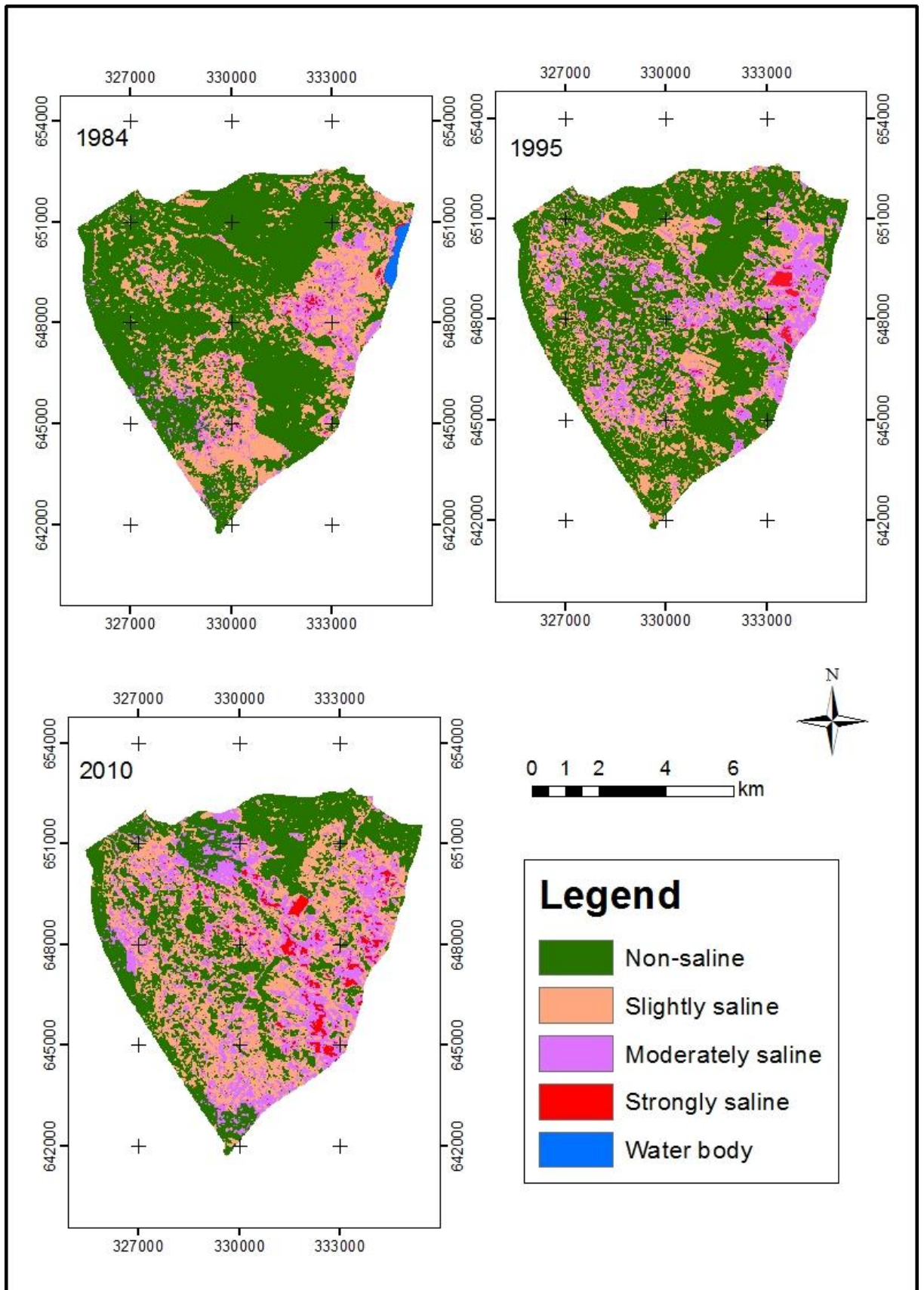


Figure 4.3 Salt affected areas derived from NDSI for 1984, 1985 and 2010

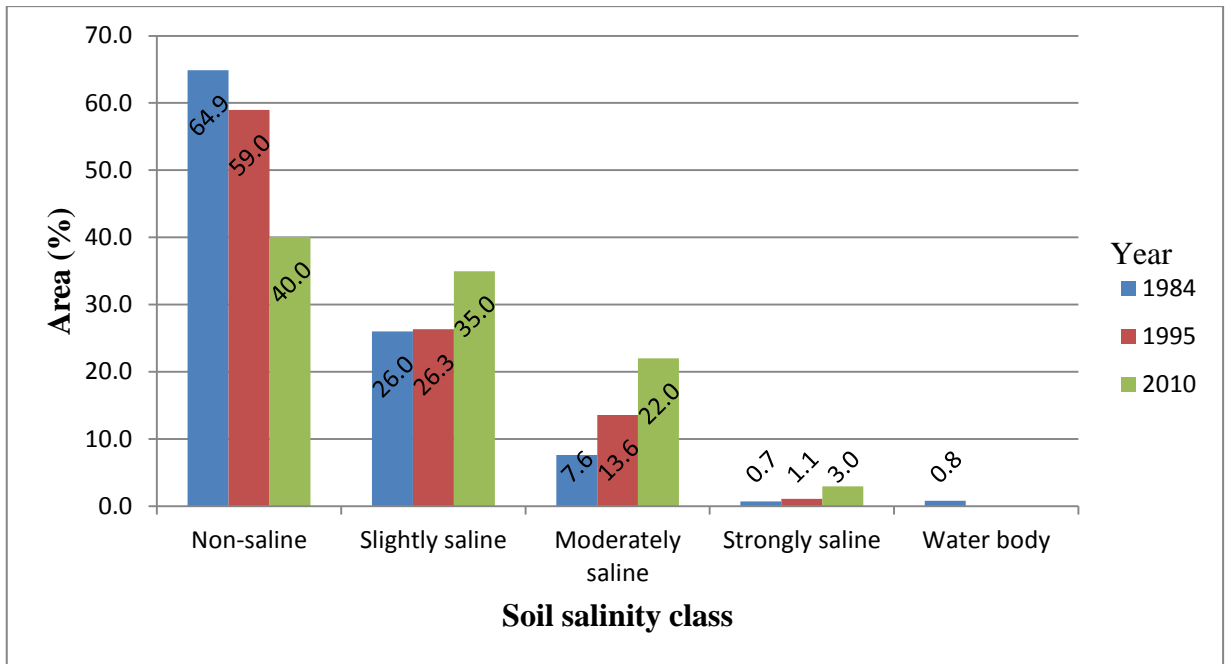


Figure 4.4 Area (%) of salt affected soils derived from NDSI for 1984, 1995 and 2010

4.3 Result of Empirical Model from Soil Salinity (ECe) and NDSI

Empirical model for the prediction of soil salinity from satellite image was developed based on soil ECe and NDSI. The derived empirical model of ECe vs NDSI has offered coefficient of determination 66.0 % (Figure 4.5). To get the salinity level at any point for the whole area directly from the image, the model was extended in ArcGIS using model builder. The derived empirical model:

$$\text{Salinity} = 58.06x^2 + 32.63x + 6.63$$

Where x is spectral reflectance/NDSI

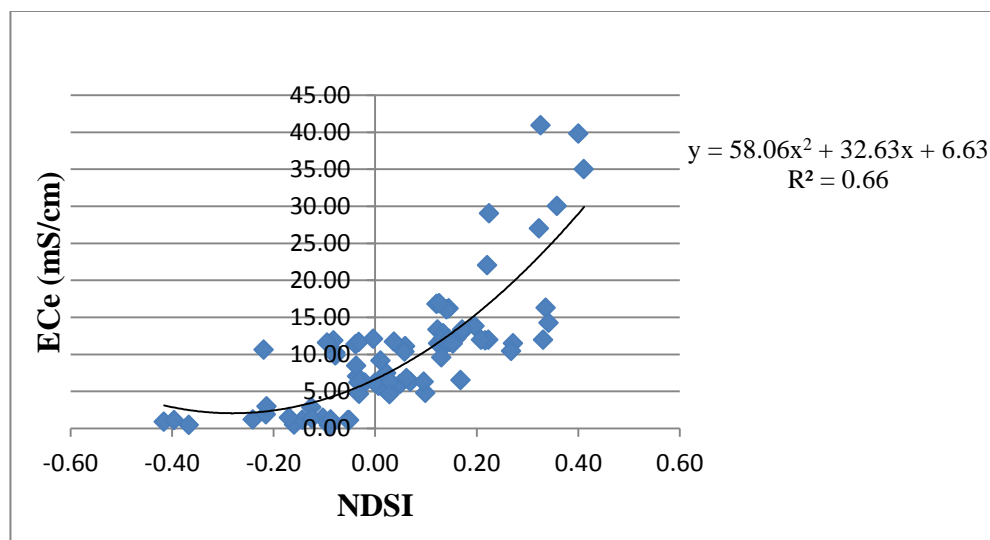


Figure 4.5 Regression analyses model between ECe and NDSI

The map of salt affected soils derived from empirical model (Figure 4.7) show that four classes of salinity level was identified with different extent of area. These were non-saline, slightly saline, moderately saline and strongly saline soils. The result shows that the non-saline soils take the largest part with an area of 3692.7 ha, which is about 54.7 % of the total area (Table 4.5). The strongly saline soil covers about 2.0 %, which is concentrated in the central part of the study area. Spatially, it coincides with those derived from supervised classification and NDSI classification except variation of areal coverage. However, the model has enhanced some new patchy areas of strong salinity in the northern and western edge of the study area. The slightly saline and moderately saline soils cover 32.6 % and 10.6 % (Figure 4.6), respectively, and are found scattered throughout the study area.

Table 4.5 Area extent of soil salinity level derived from empirical model

Salinity level (mS/cm)	Salinity Extent	Area (ha)	Area (%)
2.05-4	Non-saline	3692.7	54.7
4-8	Slightly saline	2202.0	32.6
8-15	Moderately saline	715.0	10.6
>15	Strongly saline	136.9	2.0
Total		6746.5	100.0

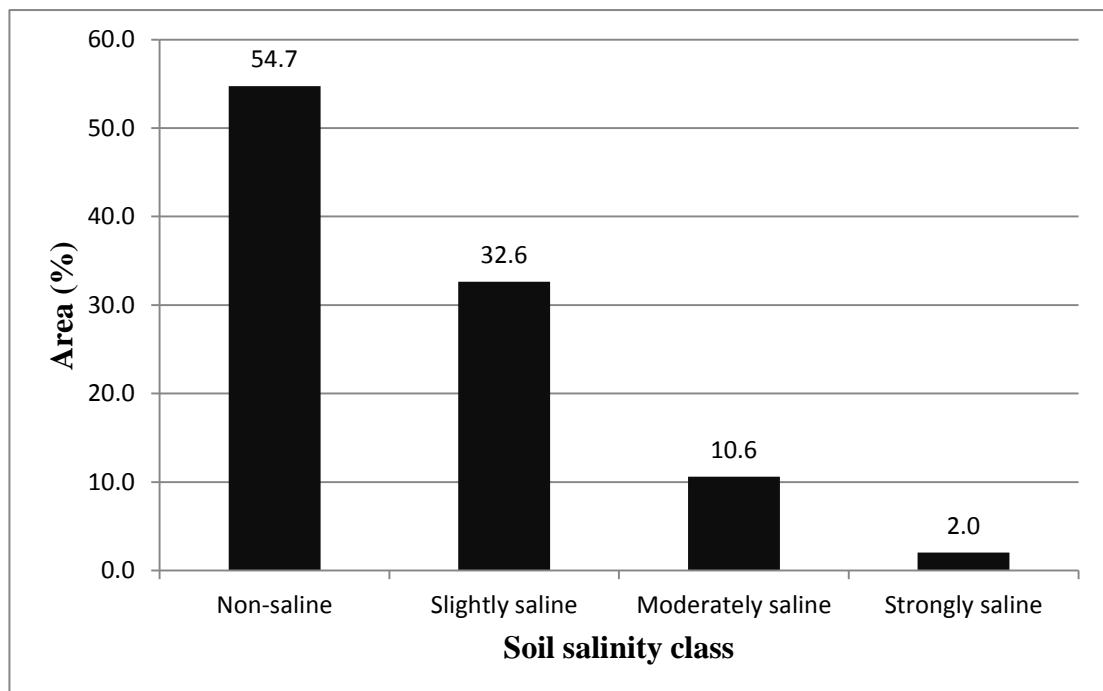


Figure 4.6 Areal extent of salt affected soils derived from empirical model

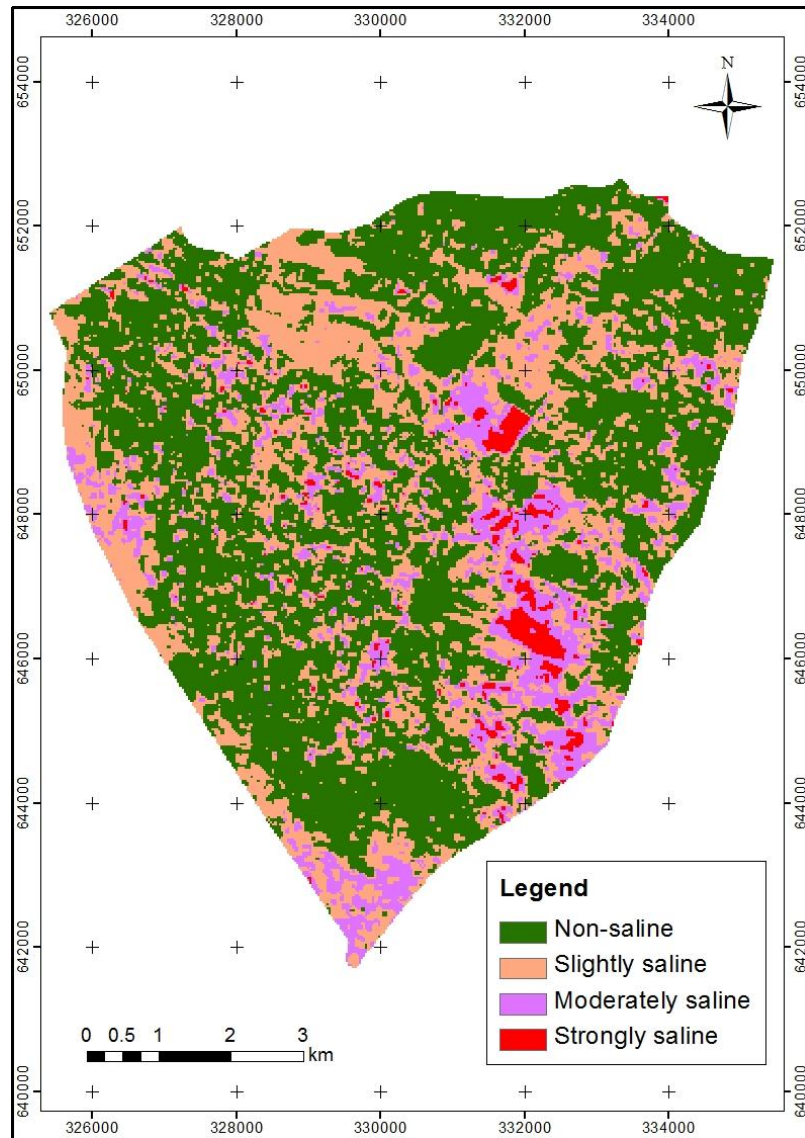


Figure 4.7 Salt affected soil map from empirical model

4.4 Result from Overlay Salinization Model

Salinity model was developed by overlaying five factor layers, which have contribution to soil salinity rise. The factors considered were water table, landform, land management type, soil texture and land cover type with varying degree of influence. Water table has higher degree of influence; about 36% followed by landform with 25% influence. Land management and land cover have 18% and 12% influence, respectively where soil texture has 9% influences.

$$\text{Salinity} = (0.36 * \text{Ground water level}) + (0.25 * \text{Landform}) + (0.18 * \text{Land management}) + (0.12 * \text{Land cover}) + (0.09 * \text{Soil texture})$$

The result of overlay soil salinization model reveals that four levels of soil salinity with varying area extent. These are the strongly saline, moderately saline, slightly saline and non-saline soils (Figure 4.9).

The result of overlay model shows most of the study area is moderately saline (Table 4.6 and Figure 4.8), which concentrated in the central and eastern part where water table level is moderate to shallow and characterized by low laying landform along the shore of Lake Chamo. This indicates that the shallow water table and low laying landforms are largely contributing to the soil salinity. Study by HALCROW-GIRDC (2009) shows that groundwater quality indicates stronger salinity levels in the lower parts of the study area, which may be due to salinization from poor water management practices or the influence of Lake Chamo on groundwater salinity near the lake shore. Consequently shallow ground water depth has higher influence on soil salinity rise and higher depth of ground water level has lower influence on soil salinization model. About 2.8% of the area is strongly saline and it is concentrated in the central part of the study area, where land management is largely under state farm and characterized by shallow water table and low laying landform. The salt free (non-saline) accounts for 26.6% where as 31.2% of the area is slightly saline. The map shows that low laying land and area with shallow water table are greatly affected by salinity.

Table 4.6 Area extent of salinity classes derived from overlay model

Salinity class	Area (ha)	Area (%)
Non-saline	1791.2	26.6
Slightly saline	2103.1	31.2
Moderately saline	2662.9	39.5
Strongly saline	189.2	2.8
Total	6746.5	100.0

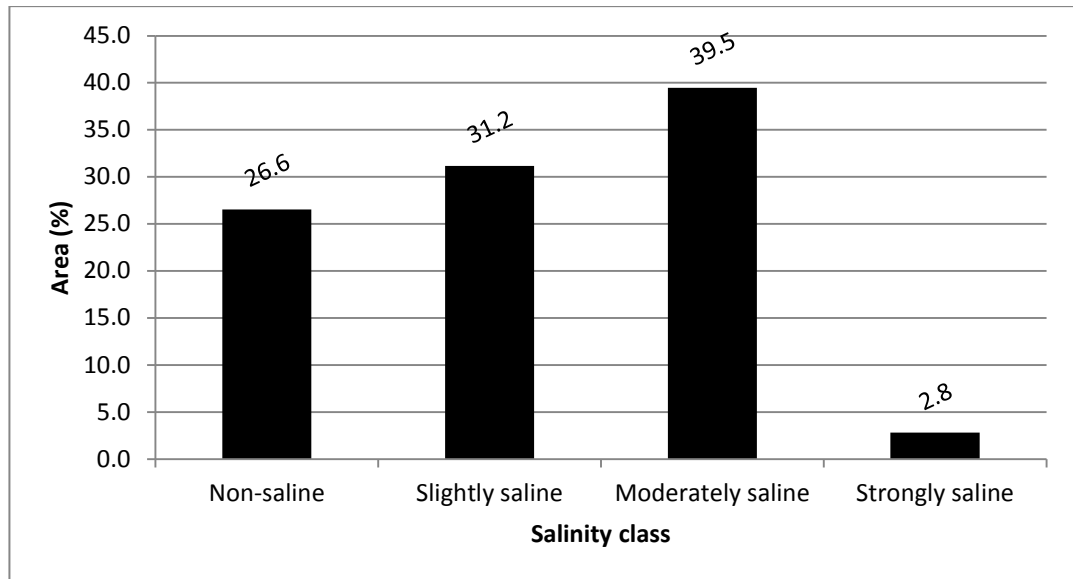


Figure 4.8 Area extent of salt affected soils from overlay model

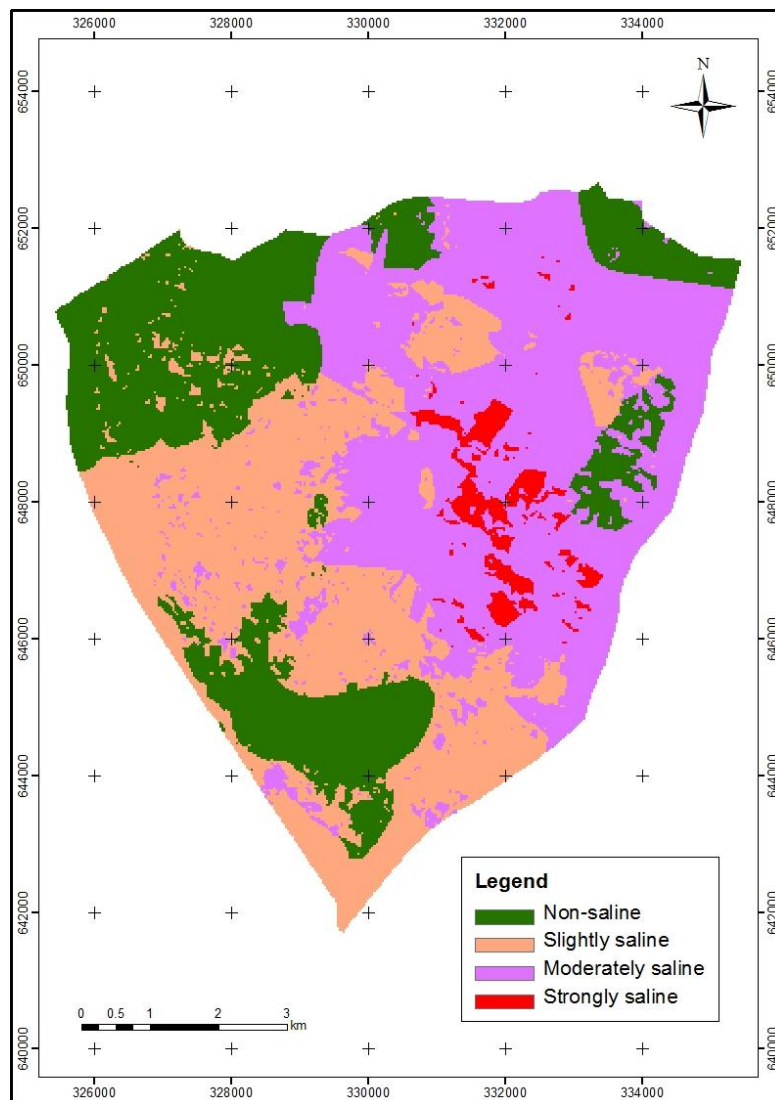


Figure 4.9 Salt affected soil map from overlay model

4.5 Validation and Comparison of the Models

Validation and comparison of empirical model derived from Soil ECe versus NDSI and overlay salinity model of the four factor layers was made. This was done by plotting the ECe value and raster value of salinity map from empirical model and overlay model on scattered diagram. Then correlation between ECe value and raster value of each of the model was derived.

The test for validity of empirical model shows that the relation between measured ECe value and salinity derived from the model has high correlation (66.0 %) (Figure 4.10). Validation for overlay model was also made and the correlation between measured ECe value and salinity derived from the model was also found correlated (68.0%) (Figure 4.11). Coefficients of correlation show that both models have approximately equal validity. However, the overlay model has better validity compared to the empirical model. Hence, prediction of salt affected areas can be executed using the overlay soil salinization model developed from the five factor layers (Water table level, landform, land management type, soil texture and land cover).

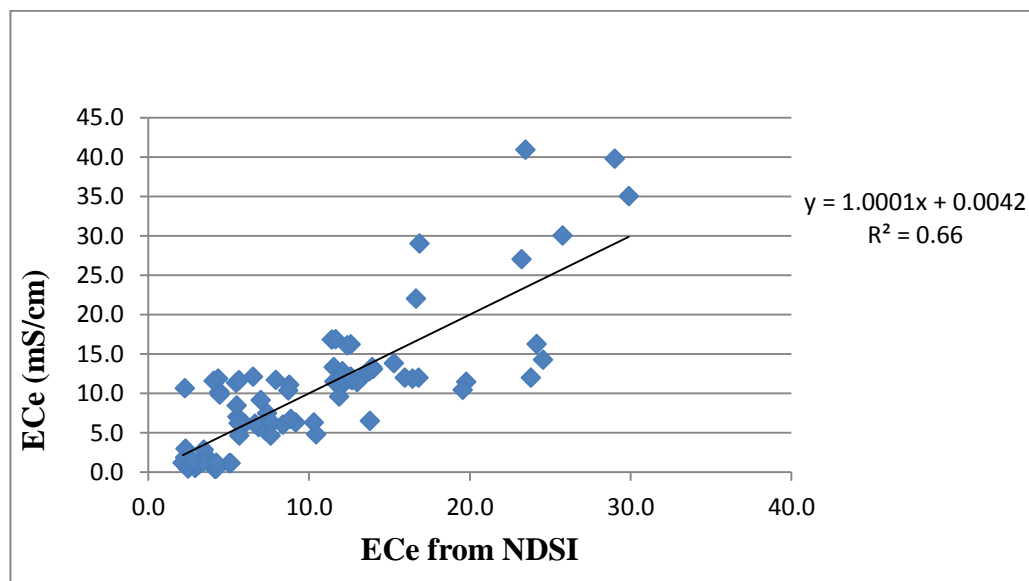


Figure 4.10 Correlation between measured ECe and ECe from empirical model

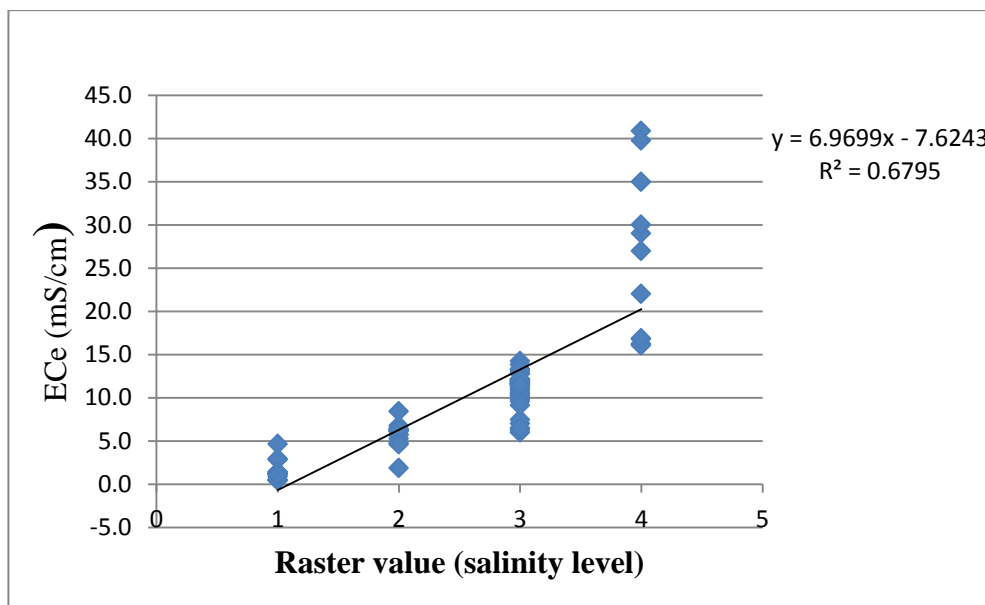


Figure 4.11 Correlation between measured ECe and raster value from overlay model (salinity level)

Field photos show the salinity status in the field. Crystalline salts were clearly seen on the land surface in some of the areas during the field visit (Plate 4.1). Currently, most of these areas are abandoned from cultivation and others left as bare land. Some areas are being used for grazing.



Plate 4.1 Photo showing surface salt crystal spread in the eastern part of the study area

4.6 Distribution of Salt Affected Areas with Respect to Water Table and Soil Type

To show spatial distribution of salt affected soil, soil type map and water table map were overlaid with the map of salt affected soils.

4.6.1 Water Table

Irrigation is the main cause of rise in shallow groundwater table under intense evapotranspiration conditions, and this led indirectly to soil salinization (Wang, et. al., 2007). Attempt was made to show areal distribution of salt affected soils with respect to water table depth. Table 4.7 shows that 13.1% of the area which is non-saline soils lay on deep water table depth whereas 8.6 % of the area was slightly saline (Under deep water table). Strongly saline soil was not identified on deep water table depth but there was small area (1.2%) with moderate salinity on deep water table depth. Out of the 3873.6 ha area, which was with shallow water table depth, about 917.9 ha and 2265.0 ha was slightly and moderately saline, respectively. The result shows that almost all the strongly saline soils covering an area of about 2.8 % is situated on shallow water table depth indicating greater contribution of ground water table to soil salinity rise.

Table 4.7 Soil salinity distribution with respect to water table depth

Water table depth	Soil salinity class								Total (ha)
	Non-saline		Slightly saline		Moderately saline		Strongly saline		
	Area (ha)	Area (%)	Area (ha)	Area (%)	Area (ha)	Area (%)	Area (ha)	Area (%)	
Deep	884.8	13.1	579.8	8.6	78.9	1.2	0.0	0.0	1543.5
Moderate	404.9	6.0	605.5	9.0	319.0	4.7	0.1	0.0	1329.4
Shallow	501.5	7.4	917.9	13.6	2265.0	33.6	189.2	2.8	3873.6
Total	1791.2	26.6	2103.1	31.2	2662.9	39.5	189.2	2.8	6746.5

4.6.2 Soil Type

The soils of the study area are primarily formed from alluvium deposited by the Sego and Sile rivers and overlies earlier lake deposits (HALCROW-GIRDC, 2009). The alluvium is composed of the weathered products of the volcanic rocks that form the catchment areas of the rivers. The area is characterized by eight major soil types: Cambisols, Fluvisols, Gleysols, Luvisols, Solonchaks, Solonetz, Vertisols and Leptosols. Map of salt affected soils were overlaid with soils type map to show its distribution. The result reveals that Cambisols dominating the study area with area extent of 3683.3 ha is largely affected with salinity where areas accounting to 19.8 % and 2.2 % are moderately and strongly saline, respectively (Table 4.8). The next salt affected soil is Fluvisols occurring in the low laying landform and it is largely under moderate salinity level accounting to 11.5 % of the area. Solonchaks and

solonetz which are associated with salt affected soils are largely under moderate salinity level with area extent of 155.4 ha (2.3%) and 138.3 ha (2.0 %), respectively, whereas the rest of the soils were slightly and strongly saline, collectively accounting for 0.6% of the area.

Table 4.8 Soil salinity distribution with respect to soil type

Soil type	Soil salinity class								Total Area (ha)
	Non-saline		Slightly saline		Moderately saline		Strongly saline		
	Area (ha)	Area (%)	Area (ha)	Area (%)	Area (ha)	Area (%)	Area (ha)	Area (%)	
Cambisols	1066.1	15.8	1136.2	16.8	1334.9	19.8	146.4	2.2	3683.6
Fluvisols	399.7	5.9	436.7	6.5	776.2	11.5	35.7	0.5	1648.4
Gleysols	10.7	0.2		0.0	36.0	0.5	0.9	0.0	47.5
Luvisols	189.3	2.8	363.2	5.4	120.6	1.8	0.3	0.0	673.4
Solonchaks	7.4	0.1	3.0	0.0	155.4	2.3	0.5	0.0	166.3
Solonetz	6.2	0.1	30.8	0.5	138.3	2.0	4.7	0.1	180.0
Vertisols	2.8	0.0	27.9	0.4	29.3	0.4	0.0	0.0	60.0
Leptosols	109.0	1.6	105.2	1.6	72.3	1.1	0.8	0.0	287.3
Total	1791.2	26.6	2103.1	31.2	2662.9	39.5	189.2	2.8	6746.5

5. Conclusion and Recommendations

5.1 Conclusion

Determination of salinization in terms of when, where and how salinity may occur is vital for sustainable production and use of soils. Thus, keeping tracking of change of salinity and predict further salinization play important roles to timely detect salinization before causing detrimental effect on the environment. Several studies and projects, using traditional or more advanced methods like remote sensing and GIS were conducted in different parts of Rift Valley Lakes basin for salinity assessment and mapping. However, they covered only the time of measurements and did not address the dynamic nature of salinity process. Hence, this study was aimed at detecting temporal and spatial distribution of soil salinity and its deriving force with the help of geospatial tools. These were done through analysis of different years of Landsat images and applying different models, which have better salinity prediction capacity for further salinization process to take proper salt affected soils management techniques.

To assess spatial and temporal variability of land cover and soil salinity, Landsat image of 1984, 1995 and 2010 was assessed under supervised classification and indices analysis. The supervised classification result showed intensive cultivation is decreasing at the rate of 58 ha/year (3.1 %/year). Fallow land is also increasing at the rate of 13 ha/year indicating abandoning of land due to salinization. On the other hand, indices analysis shows that soils under moderate and strong salinity are increasing at the rate of 37 ha/year and 6 ha/year, respectively. The analysis for NDSI also shows that slightly saline soil is increasing at a rate of 23 ha/year. Both analyses showed that soil salinization is increasing at significant rate from year to year, which may be resulted from long term irrigation as the area is under irrigated agriculture for the last three to four decades.

Two models were developed for the prediction of salt affected areas. The first model was empirical model, which were derived from the correlation of measured EC_e value and NDSI derived from Landsat image of 2010. Raster value was extracted for the corresponding EC_e value and correlation was determined where the relation was fitted into second order polynomial with R² of 66%. In most of the cases, the areas with the highest reflectance that appeared as brightest on the NDSI images had the highest EC_e. However, there were some areas with high reflectance and corresponding low EC_e values. This is because of barren land with high reflectance, but having low EC_e and this enhanced some new areas of soil salinity.

The model was extended to the whole area and map of salt affected area was derived with minimum and maximum E_{Ce} value of 2.05 mS/cm and 37.37 mS/cm, respectively. The map showed good correlation with that of derived from NDSI classification and hence the model has the capability of predicting soil salinity.

The second model was overlay model derived from five factor layers; water table, landform, land management, soil texture and land cover. The result showed that most of the strongly saline soils are on shallow water table depth (0.5 to 2 meter). Agricultural practices and excessive applications of water and fertilizer can cause soil salinization and areas where ground water table lay above critical depth increased as a result of higher evaporation and this has directly resulted in stronger salt accumulation. The model has good predictability as it considers most of the factors which contribute to soil salinization.

Validation and comparison of the two models was made to choose reliable model, which can predict areas of salt affected soils. The result shows that the overlay model has better prediction capability than the empirical model. Though the correlation coefficient between measured salinity and empirical model's salt affected map is less than that of the overlay model, it is a good and efficient method of detecting salt affected areas from satellite images.

From the overly analysis that was executed to assess spatial distribution of salt affected soils with respect to soil type, it can be concluded that most of the salt affected areas falls on Cambisols and Fluvisols, which covers larger area. Almost all of the Solonchaks and Solonetz, which are associated with saline soils, were identified as salt affected areas. The spatial distribution of salt affected soils with respect to water table showed that it is largely on shallow water table.

Generally, the results indicate that geospatial tools are efficient and feasible technique for detecting salt affected areas from satellite images and different thematic maps. It is a cost and time effective method, compared to time, labour and money spent in field work and laboratory for acquiring soil salinity data.

5.2 Recommendations

- The spatial resolution of images and DEM limit the salt affected area to be identified (small areas cannot be mapped). Hence, to maximize the accuracy of mapping salt affected soils, high resolution images and DEM should be used.

- In order to apply the empirical model to the area, there must be field visits first and adjustment and calibration because of the dynamism of salinity with time and space and sometimes similar reflectance between saline areas and barren land.
- The result shows the salt affected areas has increased in the time period considered for the study. To show the correlation between ground water level and soil salinity increase, studies on ground water level and soil salinity should be carried out at regularly intervals.
- To minimize soil salinization that arises from ground water rise as a result of irrigation water, there should be proper drainage system to remove salt and excess water.
- Crop selection should be made that are tolerant to salinity

REFERENCES

- Abbas, A. and Khan, S., 2007. Using Remote Sensing Techniques for Appraisal of Irrigated Soil Salinity.
URL:http://www.mssanz.org.au/MODSIM07/papers/46_s60/UsingRemotes60_Abbas_.pdf
- Afework Mekeberiaaw (2009). Analysis and Mapping of Soil Salinity levels in Metehara Sugarcane Estate Irrigation Farm using Different Models. Unpublished MSc Thesis. Addis Ababa University, Addis Ababa.
- Al-Khaier, F., 2003. Soil Salinity Detection Using Satellite Remote Sensing. M.Sc. Thesis. The International Institute for Geo-information Science and Earth Observation. The Netherlands, Enschede.
- Al-Mulla, Y. A., 2010. Salinity Mapping in Oman using Remote Sensing Tools: Status and Trends. A Monograph on Management of Salt-Affected Soils and Water for Sustainable Agriculture, 17-24. Sultan Qaboos University, Sultanate of Oman.
- Ali Reza, A., Sanaeinejad, S. H, Parisa, M., H, Marjan, G., Atefeh, K., 2008. Evaluation of Vegetation Cover and Soil Indices for Saline Land Classification in Neyshabour Region Using ETM+ Landsat. International Symposium on Geoinformatics for Spatial Infrastructure Development in Earth and Allied Sciences. Iran, Mashhad.
- Ashraf, S., Afshari, H., and Ebadi, A. G., 2011. Application of GIS for determination of groundwater quality suitable in crops influenced by irrigation water in the Damghan region of Iran. *International Journal of the Physical Sciences* **6**, pp. 843-854.
- Bakker, W., Janssen, L., Weir, M., Gorte, B., Pohl, C., Woldai, T., Horn, J. and Reeves, C., 2001. Principles of Remote Sensing, An Introductory Text Book. ITC, Version of 26th January.
- Beshir, A., and Bekele, S., 2007. Analysis of irrigation systems using comparative performance indicators: A case study of two large scale irrigation systems in the upper Awash basin. Oromia Water Works Design and Supervision Enterprise, IWMI-NBEA. Proceeding of the Symposium and Exhibition held at Ghion Hotel, Addis Ababa, Ethiopia. 27th -29th November 2007.

Bouksila1, F., Persson, M., Berndtsson, R., and Bahri, A., 2010. Estimating Soil Salinity Over a Shallow Saline Water Table in Semiarid Tunisia. *The Open Hydrology Journal*, 4, 91-101

Chaudhry, M.R., Ghafoor, A., Qadir, M., and Murtaza, G., 1996. Temporal variation in quality of agricultural drainage and Samundri Branch drain effluents. *Pakistan Journal of Soil Science*. 2 (1-2).

El-haddad, A., and Garcia, L.A., 2006. Detecting Soil Salinity Levels in Agricultural Lands Using Satellite Imagery.

[URL:http://proceedings.esri.com/library/userconf/proc05/papers/pap1950.pdf](http://proceedings.esri.com/library/userconf/proc05/papers/pap1950.pdf).

Elnaggar, A. A., and Noller, J. S., 2010. Application of Remote-sensing Data and Decision-Tree Analysis to Mapping Salt-Affected Soils over Large Areas. *Journal of Remote Sensing*. 2, 151-165.

HALCROW-GIRDC, 2009. Rift Valley Lakes Basin Integrated Resources Development Master Plan Study Project, Sego Irrigation and Drainage Feasibility Study Volume 3: Annexes E-I (Unpublished). Ministry of water Resource, Addis Ababa.

Jingwei Wu, Vincent, B., Yang, J., Bouarfa, S., and Vidal, A., 2008. Remote Sensing Monitoring of Changes in Soil Salinity: A Case Study in Inner Mongolia, China. *Journal of Sensors*, 8, 7035-7049.

Khan, N. M., RastosKuev, V. V., Shalina, E. V. and Sato, Y., 2001. Mapping Salt Affected Soils Using Remote Sensing Indicators-A Simple Approach with the Use of GIS IDRISI. A paper presented at 22nd Asian conference on Remote Sensing, 5-9 November 2001. Singapore.

Loiskandl, W., Ruffeis, D., Schonerkee, M., Spendlingwimmer, R., Awulachew, S. B., and Boelee, E., 2007. Case study review of investigated irrigation projects in Ethiopia. Proceeding of the Symposium and Exhibition held at Ghion Hotel, Addis Ababa. 27th -29th November 2007.

Madyaka, M., 2008. Spatial Modelling and Prediction of Soil Salinization Using SaltMod in the GIS Environment. M.Sc Thesis Submitted to International Institute for Geo-information Science and Earth Observation. The Netherlands, Enschede.

- Meiri, A. 1984. Plant Response to Salinity: Experimental methodology and application to the field. Reassessment of water quality criteria for irrigation. Soil salinity under irrigation, Ecol. Stud. Anal. Synth. **51**, 284–297.
- Mekamu Kedir, 2007. Spatial Discrimination and Mapping of Soil Salinity using Remote Sensing and GIS Techniques in the Middle Awash Basin. MSc Thesis. Addis Ababa University, Addis Ababa.
- Mongkolsawat, C. and Thirangoon, P., 1990. A Practical Application of Remote Sensing and GIS for Soil Salinity Potential Mapping in Korat Basin, Northeast Thailand. Khon Kaen University.
- Panah, S. K. A., and Zehtabian, G. R., 2002. A Database Approach for Soil Salinity Mapping and Generalization from Remotely Sensed Data and Geographic Information System. FIG XXII International Congress. Washington, D.C. April 19-26 2002.
- Patel R. M., Prasher, S. O. Bonnell, R. B. and Broughton, R. S., 2002. Development of Comprehensive Soil Salinity Index. Journal of Irrigation and Drainage Engineering. DOI: 10.1061/(ASCE)0733-9437(2002)128:3(185).
- Richard, J., 1991. Booker Tropical Soil Manual. England, pp 157-159.
- Richards L. A., 1954. Diagnosis and improvement of Saline and Alkali soils, Agriculture Handbook no. 60, United States Department of Agriculture (USDA). Washington D. C.
- Shrestha, R. P., 2006. Relating Soil Electrical Conductivity to Remote Sensing and Other Soil Properties for Assessing Soil Salinity in North East Thailand. Published online 7 August 2006 in Wiley InterScience (www.interscience.wiley.com). DOI: 10.1002/ldr.752
- Wang, Y., Xiao, D., Yan Li and Xiaoyu Li, 2007. Soil salinity evolution and its relationship with dynamics of groundwater in the oasis of inland river basins: case study from the Fubei region of Xinjiang Province, China. Environ Monit Assess. **140**:291–302

APPENDIX-I

Ground water table data of the study area taken in December 2008 and January 2009

S/N	Code	Easting	Northing	Ground water table depth (m)
1	4	332386	651883	0.5
2	6	331411	651883	1.0
3	126	330992	652515	1.8
4	137	334902	651349	1.9
5	145	333234	651748	1.8
6	166	330008	651491	1.2
7	201	331507	651244	1.9
8	221	334252	650748	0.7
9	229	332248	650748	2.0
10	267	334749	650250	1.1
11	291	332754	650005	1.8
12	325	330008	649506	1.3
13	332	331750	649500	1.5
14	345	334502	649252	1.7
15	387	330956	648724	2.0
16	394	328751	648751	0.7
17	396	326506	648498	2.0
18	398	327504	648487	1.2
19	414	331999	648497	1.2
20	425	334250	648250	2.0
21	430	333000	648250	2.0
22	444	329250	648250	2.0
23	461	334250	647752	1.5
24	464	333483	647754	2.0
25	467	332752	647750	1.5
26	474	330988	647754	1.8
27	478	330001	647748	1.3
28	518	332000	647250	1.6
29	522	331000	647251	1.4
30	526	330001	647247	2.0
31	529	328752	647264	1.2
32	562	327997	646501	1.2
33	563	328498	646494	1.6
34	581	332988	646491	1.8
35	594	331782	646263	1.7
36	634	327999	645494	1.7
37	643	330500	645500	1.8

S/N	Code	Easting	Northing	Ground water table depth (m)
38	657	333000	645247	1.8
39	670	329749	645251	1.6
40	699	328996	644499	1.9
41	702	329741	644490	1.5
42	912	334347	649892	2.5
43	914	333078	649177	1.5
44	915	333500	650750	1.7
45	916	334537	651719	3.3
46	925	329478	651818	1.9
47	928	330523	646249	4.0
48	929	331996	645746	4.0
49	932	330374	641973	3.5
50	934	327992	649480	3.5
51	997	329748	645885	3.5

APPENDIX-II

Accuracy assessments of land cover map of 2010 (Figure 4.1).

Class	Ground control points					Total	User accuracy %
	Bare land	Intensive cultivation	Fallow	Dispersed cultivation	Water body/Swamp		
Bare land	12	1	1	2	0	16	75.0
Intensive cultivation	1	18	0	2	0	21	85.7
Fallow	1	1	14	1	0	17	82.4
Dispersed cultivation	0	3	0	25	1	29	86.2
Water body/Swamp	0	0	0	0	2	2	100.0
Total	14	23	15	30	3	85	
Producer accuracy %	85.7	78.3	93.3	83.3	66.7		83.5

APPENDIX-III

Soils saturated extract Electrical conductivity (ECe) and pH data analysed from auger samples of 2009.

S/N	Auger No	Easting	Northing	Ece 1:5 (mS/cm)	pH 1:5	Salinity overlay model result
1	17	327316	650646	0.4	7.1	Non-saline
2	43	327816	649646	0.4	7.0	Non-saline
3	98	329482	645989	5.7	7.1	Slightly saline
4	140	334408	651541	6.4	8.3	Slightly saline
5	141	334861	650917	12.8	8.1	Moderately saline
6	145	333398	651710	5.7	7.7	Slightly saline
7	151	331655	651543	11.6	7.7	Moderately saline
8	153	331155	651543	11.1	8.2	Moderately saline
9	157	329589	651484	11.6	8.3	Moderately saline
10	163	328343	651574	0.5	7.6	Non-saline
11	167	330157	651288	6.1	8.1	Slightly saline
12	169	328050	647944	7.0	7.9	Moderately saline
13	171	331159	651289	12.1	7.9	Moderately saline
14	182	326917	647718	6.0	8.7	Moderately saline
15	183	333620	650974	13.3	8.1	Moderately saline
16	185	334722	651324	4.6	7.5	Non-saline
17	190	334441	651260	7.5	3.9	Moderately saline
18	194	333155	651043	11.5	8.1	Moderately saline
19	200	331648	651044	11.5	8.3	Moderately saline
20	202	331156	651050	11.9	8.0	Moderately saline
21	208	330655	650793	6.2	8.7	Slightly saline
22	210	331655	650793	12.0	8.2	Moderately saline
23	213	333155	650793	9.8	7.6	Moderately saline
24	215	333793	652138	6.3	8.1	Moderately saline
25	219	334656	650541	12.0	8.3	Moderately saline
26	220	334083	651737	6.5	8.5	Moderately saline
27	223	330281	647777	16.3	7.6	Strongly saline
28	225	333155	650543	16.2	8.2	Strongly saline
29	233	331158	650547	10.3	8.1	Moderately saline
30	237	330192	650259	12.1	7.9	Moderately saline
31	238	325903	650293	0.4	8.4	Non-saline
32	244	328595	650090	1.2	7.5	Non-saline
33	246	329915	650309	6.3	7.8	Slightly saline
34	248	332086	650386	12.1	8.0	Moderately saline
35	250	330907	650291	12.2	8.2	Moderately saline
36	252	330629	650318	6.1	8.3	Slightly saline
37	261	333655	650293	11.3	8.3	Moderately saline
38	263	334149	650296	10.4	4.2	Moderately saline

S/N	Auger No	Easting	Northing	Ece 1:5 (mS/cm)	pH 1:5	Salinity overlay model result
39	275	332690	650020	11.7	8.8	Moderately saline
40	284	330405	650043	10.9	7.7	Moderately saline
41	289	331656	649794	12.8	8.0	Moderately saline
42	291	332659	649798	9.6	7.4	Moderately saline
43	298	334655	649533	11.9	8.0	Moderately saline
44	300	334155	649538	29.0	8.4	Strongly saline
45	318	326412	649308	0.9	3.9	Non-saline
46	322	328357	649383	1.2	8.1	Non-saline
47	336	332658	649294	14.2	10.0	Moderately saline
48	337	332904	649281	11.4	10.2	Moderately saline
49	349	333403	649046	13.8	8.0	Moderately saline
50	361	330392	649038	6.8	7.9	Slightly saline
51	369	333155	648793	8.4	7.4	Slightly saline
52	383	331905	648543	11.6	7.8	Moderately saline
53	393	329154	648543	1.9	7.8	Slightly saline
54	399	327109	648996	1.1	8.4	Non-saline
55	423	334123	648282	11.6	9.3	Moderately saline
56	426	333905	648043	9.2	8.2	Moderately saline
57	427	330678	646958	11.8	7.6	Moderately saline
58	430	332905	648043	10.2	7.7	Moderately saline
59	438	329501	649222	4.8	8.6	Slightly saline
60	444	329370	649809	1.4	8.0	Non-saline
61	453	332142	647783	11.7	8.0	Moderately saline
62	458	333908	647795	16.1	8.2	Strongly saline
63	467	332631	647537	40.9	7.2	Strongly saline
64	469	330259	646209	6.3	7.9	Slightly saline
65	502	332403	647294	12.0	7.6	Moderately saline
66	506	333404	647294	16.8	7.8	Strongly saline
67	507	333656	647295	27.0	8.1	Strongly saline
68	517	329424	645789	4.6	3.5	Slightly saline
69	539	333652	646547	13.3	6.9	Moderately saline
70	541	333154	646540	10.6	7.7	Moderately saline
71	547	331655	646543	22.0	7.8	Strongly saline
72	549	329632	646801	13.1	8.2	Moderately saline
73	558	325957	648834	1.1	7.6	Non-saline
74	581	333135	646273	35.0	7.3	Strongly saline
75	586	332925	646164	39.8	7.8	Strongly saline
76	589	332023	646310	30.0	7.9	Strongly saline
77	591	331626	645418	5.3	7.6	Slightly saline
78	595	327770	646730	2.9	7.7	Non-saline
79	655	332905	645040	16.9	9.9	Strongly saline
80	674	329700	643844	2.8	7.8	Non-saline
81	682	332152	644544	1.3	7.7	Non-saline

S/N	Auger No	Easting	Northing	Ece 1:5 (mS/cm)	pH 1:5	Salinity overlay model result
82	718	327983	644675	1.4	7.4	Non-saline
83	724	328420	644001	1.2	7.6	Non-saline
84	781	330159	643291	1.1	7.6	Non-saline

DECLARATION

I hereby declare that the dissertation entitled “**Mapping of Soil Salinity in Sego Irrigation Farm, Southern Ethiopia, using Geospatial Tools**” has been carried out by me under the supervision of Dr. K. V. Suryabhagavan, Department of Earth Sciences, Addis Ababa University, Addis Ababa during the year 2011-2012 as a part of Master of Science programme in Geo-information Science. I further declare that this work has not been submitted to any other University or Institution for the award of any degree or diploma.

Zewdu Shegena

Signature _____

Place: Addis Ababa

Date: June 2012

CERTIFICATE

This is certified that the dissertation entitled “**Mapping of Soil Salinity in Sego Irrigation Farm, Southern Ethiopia, using Geospatial Tools**” is a bonafied work carried out by Zewdu Shegena under my guidance and supervision. This is the actual work done by Zewdu Shegena for the partial fulfilment of the award of the Degree of Master of Science in Geo-information Science from Addis Ababa University. Addis Ababa.

Dr. K. V. Suryabhagavan

Assistant Professor

Signature _____

Department of Earth Sciences

Addis Ababa University

Addis Ababa